

AD _____

Award Number: W81XWH-12-2-0035

TITLE: Gram-Negative Bacterial Wound Infections

PRINCIPAL INVESTIGATOR: Luis A. Actis

CONTRACTING ORGANIZATION: Miami University, Oxford, OH 45056

REPORT DATE: May 2014

TYPE OF REPORT: Annual

PREPARED FOR: U.S. Army Medical Research and Materiel Command
Fort Detrick, Maryland 21702-5012

DISTRIBUTION STATEMENT: Approved for Public Release;
Distribution Unlimited

The views, opinions and/or findings contained in this report are those of the author(s) and should not be construed as an official Department of the Army position, policy or decision unless so designated by other documentation.

REPORT DOCUMENTATION PAGE				<i>Form Approved</i> OMB No. 0704-0188	
Public reporting burden for this collection of information is estimated to average 1 hour per response, including the time for reviewing instructions, searching existing data sources, gathering and maintaining the data needed, and completing and reviewing this collection of information. Send comments regarding this burden estimate or any other aspect of this collection of information, including suggestions for reducing this burden to Department of Defense, Washington Headquarters Services, Directorate for Information Operations and Reports (0704-0188), 1215 Jefferson Davis Highway, Suite 1204, Arlington, VA 22202-4302. Respondents should be aware that notwithstanding any other provision of law, no person shall be subject to any penalty for failing to comply with a collection of information if it does not display a currently valid OMB control number. PLEASE DO NOT RETURN YOUR FORM TO THE ABOVE ADDRESS.					
1. REPORT DATE May-2014		2. REPORT TYPE Annual		3. DATES COVERED 1 May 2013 - 30 April 2014	
4. TITLE AND SUBTITLE Gram-negative bacterial wound infections				5a. CONTRACT NUMBER W81XWH-12-2-0035	
				5b. GRANT NUMBER W81XWH-12-2-0035	
				5c. PROGRAM ELEMENT NUMBER	
6. AUTHOR(S) Luis A. Actis Betty Diamond E-Mail: actisla@miamioh.edu				5d. PROJECT NUMBER	
				5e. TASK NUMBER	
				5f. WORK UNIT NUMBER	
7. PERFORMING ORGANIZATION NAME(S) AND ADDRESS(ES) Miami University. 501 E High Street, Oxford, OH 45056				8. PERFORMING ORGANIZATION REPORT NUMBER	
9. SPONSORING / MONITORING AGENCY NAME(S) AND ADDRESS(ES) U.S. Army Medical Research and Materiel Command Fort Detrick, Maryland 21702-5012				10. SPONSOR/MONITOR'S ACRONYM(S)	
				11. SPONSOR/MONITOR'S REPORT NUMBER(S)	
12. DISTRIBUTION / AVAILABILITY STATEMENT Approved for Public Release; Distribution Unlimited					
13. SUPPLEMENTARY NOTES					
14. ABSTRACT Biochemical and functional analyses of the <i>A. baumannii</i> AB5075 wild type parental strain and isogenic insertion derivatives showed that inactivation of genes coding for biosynthesis and transport of the high-affinity siderophore acinetobactin drastically affects the capacity of this strain to grow under iron-limiting laboratory conditions as well as to infect and kill <i>G. mellonella</i> larvae and BALB/c mice in experimental infection assays. These results validate AB5075 as a proper model strain to study virulence under <i>in vitro</i> and <i>in vivo</i> conditions and demonstrate the central role the acinetobactin-mediated iron acquisition system plays in its virulence. Equally relevant is the finding that all <i>A. baumannii</i> wound isolates tested were sensitive to Ga-PPIX independent of the composition of the media. These observations support our goal of using this non-ferric metalloporphyrin derivative as an anti-microbial agent in a wound infection model. Such an approach is feasible because Ga-PPIX does not display detectable cell and animal toxicity within the concentration range we plan to test based on data obtained with other pathogens. Although these observations are encouraging regarding the potential use of Ga-PPIX as an alternative to treat infections caused by MDR <i>A. baumannii</i> strains, the efficacy of this non-ferric metalloporphyrin derivative against other wound pathogens is not conclusive and requires some additional studies. Similar conclusions were obtained using gallium nitrate, the activity of which depends on the composition of the media. The successful implementation of a tissue culture model, which examines critical host-pathogen interactions, has the potential for providing novel and critical information on the pathobiology of bacteria that cause severe human infections.					
15. SUBJECT TERMS					
16. SECURITY CLASSIFICATION OF:			17. LIMITATION OF ABSTRACT	18. NUMBER OF PAGES	19a. NAME OF RESPONSIBLE PERSON
a. REPORT U	b. ABSTRACT U	c. THIS PAGE U			USAMRMC
			UU	36	19b. TELEPHONE NUMBER (include area code)

Table of Contents

	<u>Page</u>
Introduction.....	4
Body.....	4
Key Research Accomplishments.....	9
Reportable Outcomes.....	9
Conclusions.....	10
References.....	10
Appendices.....	11
Supporting data.....	12

Introduction

The overall purpose of this research effort is to determine the role iron acquisition and biofilm functions expressed by Gram-negative pathogens play in the pathogenesis of severe infections in the Wounded Warrior because of polytrauma and blast injuries. The information collected with these studies will be used to explore the efficacy of different chemical and biological agents to block these potential virulence functions using appropriate experimental infection models. These studies have the potential of providing not only new basic information on the pathobiology of bacteria that cause serious infections, but also facilitating the development of new and more effective therapeutics to treat severe Gram-negative infections in wounded military personnel.

Body

Expression of iron uptake functions

Data collected during the first year of this project led us to the selection of *A. baumannii* AB5075 as the type strain to be used for further study. This strain, which was isolated from a wounded soldier, was selected from the Multidrug-Resistant Organism Repository and Surveillance Network (MRSN) strain collection at the Walter Reed Army Institute of Research (WRAIR). Functional and chemical assays showed that AB5075 produces catechol-based siderophore(s), which allows it to grow under iron-chelated conditions. To further characterize the iron uptake proficiency of AB5075, we used isogenic random transposon insertion derivatives generated by Drs. Daniel V. Zurawski (WRAIR) and Colin Manoil (University of Washington Genome Sciences, Seattle, WA) using the *in vitro* Transposome insertion system developed by Epicentre, which we used before with the *A. baumannii* ATCC 19606^T strain (1). This approach resulted in the identification of AB5075 mutants 3320 (*bauA::Tn*) and 3340 (*entA::Tn*) with a single insertion in the *bauA* and *entA* genes. The *bauA* gene codes for the acinetobactin outer membrane receptor protein BauA (2), while *entA* codes for the EntA enzyme that is required for the biosynthesis of dihydroxybenzoic acid (DHBA), an essential precursor for acinetobactin production (3). Arnow colorimetric assays were negative with AB5075 succinate-based cultures supernatants and reverse-phase high performance liquid chromatography (RP-HPLC) analysis of M9 minimal medium culture supernatants showed that the AB5075 3340 derivative produces neither DHBA nor fully mature acinetobactin (Fig. 1). This result is identical to that obtained with the ATCC 19606^T derivative 3060, which was used as a control because it harbors an insertion in *entA* (3). The immunoblotting analysis of cell lysates prepared from the AB5075 3320 BauA mutant proved that this derivative does not produce the BauA acinetobactin outer membrane receptor protein. These assays correlated with the observation that the inactivation of the *entA* and *bauA* genes results in a drastic impairment of the iron acquisition capacity of AB5075 when cultured in media containing increasing concentrations of the synthetic iron chelator 2,2'-dipyridyl (DIP) (Fig. 2). These observations are a clear indication that *A. baumannii* AB5075 is capable to grow under iron-chelated conditions as long as it produces and uses the high-affinity siderophore acinetobactin we described in the ATCC 19606^T strain (2). These results together with data we already published (3) and collected during the first year of this award also support the observation that the acinetobactin-mediated iron acquisition system is the most common iron uptake system expressed by different *A. baumannii* clinical isolates.

In addition to the production and utilization of acinetobactin, we examined the possibility that *A. baumannii* uses siderophores produced by other pathogens (xenosiderophores) as it may happen in poly-microbial infections. This hypothesis is supported by the observation that the genome of different *A. baumannii* strains harbor genes coding for the transport of other siderophores, such as enterobactin. For this purpose, we used the *A. baumannii* ATCC 19606^T *bauA* and *entA* mutants as reporter strains in cross-feeding assays we have described before (2, 3). These two well-characterized mutants, which are impaired in acinetobactin-mediated iron uptake (2, 3), were incubated under iron-chelated conditions in the presence of iron-deficient cell-free culture supernatants prepared from *Pseudomonas aeruginosa* (5 strains), *Klebsiella pneumoniae* (6 strains) and *Escherichia coli* (6 strain) strains. These 17 multidrug resistant (MDR) isolates, which were obtained from wounded military personnel and sent to us by our collaborator Dr. D. Zurawski (WRAIR), proved to be iron uptake proficient and produce siderophores when cultured under chelated conditions (Table 1). Siderophore cross-feeding assays using cell-free culture supernatants of some of these 17 strains showed that the ATCC 19606^T *bauA* and *entA* mutants grow under iron-chelated conditions in the presence of *K. pneumoniae* and *E. coli* iron-restricted culture supernatants, although these two mutants do not use or produce the native acinetobactin siderophore (Table 2). In contrast, none of the *P. aeruginosa* culture supernatants tested recovered the growth of the ATCC 19606^T iron acquisition reporter mutants.

These observations and our previous publications (2-4) indicate that *A. baumannii* strains, including those isolated from wounded military personnel, are iron-uptake proficient and capable of using siderophores they produce as well as siderophores produced by other pathogens. Although this finding is not novel considering the fact that other bacterial pathogens display a similar response, the utilization of xenosiderophores, which has not been described for *A. baumannii* so far, poses a treatment challenge in cases where wounded soldiers are infected by more than one pathogen. Therefore, targeting a particular iron acquisition system, such as the acinetobactin system expressed by most *A. baumannii* studied strains, may not be an effective therapeutic approach. Thus, the development of alternatives based on the inhibition of more general/universal rather than specific iron acquisition and metabolic functions could be a more practical and relevant route, as described below in the analysis of the effects of gallium (Ga)-containing compounds on bacterial growth.

Inhibition of iron uptake functions

Siderophore biosynthesis inhibitors

Work conducted during the first year of this award showed that potential siderophore inhibitors, including sodium salicylate, 5-chlorosalicylic acid, salicylamide, diflunisal, 5-sulfosalicylic acid, 2-hydroxy-5-nitrobenzoic acid, 5-aminosalicylic acid, and 4-aminosalicylic acid, had no detectable effect on the growth of *A. baumannii* under iron-chelated conditions or required high concentrations to obtain a detectable growth inhibitory effect. Furthermore, a recent report showed that a series of non-nucleoside inhibitors of BasE, an essential acinetobactin biosynthetic enzyme, do not have detectable growth inhibitory effects when *A. baumannii* is cultured in their presence under chelated conditions, although these inhibitors strongly interact with this enzyme (5). All these observations indicate that the inhibition of biosynthetic components involved in siderophore production may not be a viable approach to treat infections caused by *A. baumannii* MDR strains. These observations also prompted us to test Ga derivatives since this element does not have the iron redox properties essential for cell physiology, have been used in human medicine and may affect intracellular bacterial iron metabolism rather than the acquisition of this metal.

Gallium nitrate [Ga(NO₃)₃] growth inhibitory effects

Study of *A. baumannii* strains

Based on the considerations presented above and data we previously published (6), we tested the susceptibility of 43 *A. baumannii* strains, which included, in addition to the 29 MRSN *A. baumannii* strains, 14 isolates representing different clonal type strains, 10 strains whose genomes were fully sequenced and annotated as well as strains that were classified as antimicrobial sensitive or MDR, using a carefully designed systematic approach. Although all tested strains displayed minimal growth after 24 h incubation in M9 minimal medium containing 100 μ M DIP, we observed a variable Ga(NO₃)₃ susceptibility response among them. Table 3 shows that some of the isolates, such as strains 406 and 2886, were sensitive to 125 μ M Ga(NO₃)₃ when compared with the cognate sample containing no Ga(NO₃)₃. On the other hand, other isolates, such as strain 3158, showed no significant growth differences in the presence or absence of Ga(NO₃)₃. Furthermore, several strains displayed more growth at the highest Ga(NO₃)₃ concentrations than intermediate concentrations. Since the effect of Ga(NO₃)₃ depends on iron chelation, the varying results we observed among different *A. baumannii* strains may relate to differences in the capacity of each isolate to acquire iron under limiting conditions. Furthermore, it is possible that the laboratory conditions we used to conduct these studies do not reflect the growth inhibitory capacity of Ga(NO₃)₃ in an *in vivo* model. Thus, we will test the antimicrobial efficacy of Ga(NO₃)₃ using a selected set of *A. baumannii* strains in the *G. mellonella* virulence assays we recently used to test the virulence role of *A. baumannii* iron acquisition (4) during the next year of the award.

Study of other wound pathogens

We also examined the antimicrobial effect of Ga(NO₃)₃ on other pathogens different from *A. baumannii*. For this purpose we compared the response of the MRSN *K. pneumoniae* strain 4640, which was selected by Dr. Zurawski as the working strain, to that of the *A. baumannii* ATCC 19606^T and AB5075, which we showed are sensitive to this gallium salt when incubated under iron-limiting conditions. *K. pneumoniae* 4640 has a response similar to that displayed by the ATCC 19606^T and AB5075 strains; its growth is affected by Ga(NO₃)₃ in a dose-dependent manner when bacteria are cultured under iron-chelated conditions generated by the presence of 100 μ M DIP. These results indicate that wound pathogens different from *A. baumannii* are susceptible to Ga(NO₃)₃ under the iron-limiting conditions they most likely encounter in the human host. We will extend these studies by analyzing all *E. coli*, *K. pneumoniae* and *P. aeruginosa* MRSN isolates during the next year of the award using standard microbiology laboratory conditions as well as *in vivo* conditions with the *G.*

mellonella virulence model. These studies should provide a more comprehensive understanding of the inhibitory effects of Ga(NO₃)₃ under conditions that would mimic those found by these pathogens in medical settings and the human host.

Ga-protoporphyrin IX (Ga-PPIX) growth inhibitory effects

Study of *A. baumannii* strains

Non-ferric metalloporphyrin derivatives, particularly Ga-protoporphyrin IX (Ga-PPIX), proved to be effective antimicrobials when tested against a wide range of bacteria (7). Therefore, we determined whether the 41 strains used to test the effect of Ga(NO₃)₃ (Table 3) were also sensitive to Ga-PPIX using a similar approach. Table 4 shows that the presence of Ga-PPIX affected the growth of all tested strains in a dose-dependent manner, with concentrations ≥ 62.5 μM producing the highest growth inhibitory effects. Results obtained with disk diffusion assays, which are more convenient than microdilution assays for testing a large number of clinical isolates, showed a good correlation with the data collected using microdilution assays. The detailed analysis of AB5075 (strain #3156 in Table 4) showed a Ga-PPIX minimal inhibitory concentration (MIC) of 31.25 μM when cultured in standard Mueller-Hinton broth or agar used for this purpose (Fig. 3, panels A and B). The Ga-PPIX susceptibility of strain AB5075 was not significantly affected by growing it on Luria-Bertani, Mueller-Hinton or Brain Heart Infusion (BHI) agar (Fig. 4) or the presence of free iron or DIP in the medium (data not shown). Finally, the comparative analysis of *A. baumannii* ATCC 19606^T, an old isolate that is not extensively drug resistant, with the strains AB3785 and AB5075, which are considered contemporary MDR wound isolates, showed that the antibiotic resistance phenotype and the time of their isolation do not affect their susceptibility to Ga-PPIX.

Overall, these results indicate that Ga-PPIX is an effective antimicrobial agent that affects bacterial growth independently of the composition and iron content of different culture media as well as the antibiotic resistance phenotype of different *A. baumannii* clinical isolates. This seems to be a significant advantage over the growth inhibitory effects caused by Ga(NO₃)₃.

Study of other wound pathogens

Since published data (7, 8) and the observations described in the previous paragraph indicate that Ga-PPIX has the potential to affect the growth of different bacterial pathogens, we tested the susceptibility of extended-spectrum β-lactamase (ESBL)-producing *E. coli* strains isolated from wounded soldiers and provided to us by Dr. Zurawski (Table 1). Disk diffusion assays showed that not all strains displayed the same susceptibility to Ga-PPIX when cultured on LB agar containing the synthetic iron chelator 2,2'-dipyridyl (DIP). For example, strains 105454 and 105438 were more sensitive to Ga-PPIX than strains 109497 and 105547, the latter of which was the least sensitive. These results indicate that different bacterial pathogens may display different susceptibility to this non-ferric metalloporphyrin derivative. This hypothesis is supported by the observation that none of the *E. coli*, *K. pneumoniae* and *P. aeruginosa* MRSN strains were sensitive Ga-PPIX when cultured in LB and only the *E. coli* strains 105454, 105547, 109497 and 105438 were Ga-PPIX sensitive when cultured under iron-chelated conditions imposed by the presence of DIP (Table 5). The fact that iron chelation is required to affect viability of *E. coli* under aerobic conditions suggests that Ga-PPIX may be viable for treatment of wound infections and/or complement to hyperbaric treatment. *K. pneumoniae*'s and *P. aeruginosa*'s lack of susceptibility may be because iron chelation was not sufficient to induce the expression of heme uptake functions, which may be required for the uptake of Ga-PPIX needed for cell toxicity. Taken together, these results illustrate the differences in heme metabolism amongst bacteria belonging to these genera as well as potential concerns regarding the universality of iron metabolism inhibitors, which could be used therapeutically to treat different wound pathogens.

Role of iron uptake functions in the virulence of AB5075

Galleria mellonella infection model

We showed that the ability of the *A. baumannii* ATCC 19606^T type strain to interact with and damage human alveolar epithelial cells as well as to kill an invertebrate host, such as *G. mellonella* caterpillars, or mice depends on the expression of a fully active acinetobactin-mediated iron acquisition system (4). In addition, we showed in previous quarter reports that *A. baumannii* AB5075 produces and uses acinetobactin when cultured in standard bacteriological media containing DIP. These observations prompted us to compare the virulence of the AB5075 wild type strain with that of AB5075 isogenic mutants affected in the expression of *entB* and *bauA*, which were generated and analyzed as describe before in this report. Figure 5 shows that the injection of *G.*

mellonella with 10^5 cells of the AB5075 strain killed approximately 50% of larvae 120 h (5 days) after infection. This death rate is similar to that we previously reported for larvae injected with the *A. baumannii* ATCC 19606^T type strain (4). In contrast, infection of larvae with 10^5 cells of the AB5075 *bauA::Tn* or *entB::Tn* isogenic mutants resulted in death rates statistically indistinguishable from the control animals, which were injected with sterile phosphate-buffered saline (PBS) solution, but significantly lower than the killing rate of the AB5075 wild type parental strain.

Mouse pneumonia model

This infection model has been used to assess the virulence of different *A. baumannii* strains (9) including the virulence of the AB5075 strain we report in the manuscript recently accepted for publication in mBio (see appendix 4). Figure 6 shows that almost 90% of the cyclophosphamide immunosuppressed BALB/c mice infected with the AB5075 wild type strain died 96 h after infection with 1.4×10^6 colony forming units (CFUs). In contrast, the infection of the animals with 1.6×10^6 or 1.3×10^6 CFUs of the AB5075 *bauA::Tn* or *entA::Tn* mutants, respectively, resulted in a drastic virulence reduction when compared with that of the parental strain and indistinguishable from the negative control injected with sterile PBS. These results reflect our observations obtained with the ATCC 19606^T strain, which also showed that the active production and utilization of acinetobactin as an iron source is critical for *A. baumannii* virulence (4).

Taken together, these *in vivo* observations not only validate the *G. mellonella* infection model using two unrelated *A. baumannii* strains (ATCC 19606^T and AB5075), but also demonstrate that the virulence of *A. baumannii* AB5075 depends on the expression of active iron acquisition functions in animals that present iron limiting conditions similar to those this pathogen encounters in the human host. It is also apparent from these results that, like the ATCC 19606^T strain, the expression of the acinetobactin-mediated system is the main mechanisms by which AB5075 acquires iron. All these observations support our hypothesis that blocking the production and/or utilization of acinetobactin or affecting intracellular iron metabolism is a reasonable approach to develop alternative therapeutics to treat infections caused by MDR pathogens including *A. baumannii* isolated from wounded military personnel.

Targeting iron utilization functions in AB5075

Ga-PPIX animal and cell toxicity

Considering the bacterial growth inhibitory effect that Ga-PPIX displayed when tested using laboratory conditions, we decided to extend these studies by using biologically relevant and convenient experimental models, such as A549 human alveolar epithelial monolayers and the *G. mellonella* infection model to obtain preliminary data before moving into murine infection models. We started these studies by testing the cell and animal toxicity of Ga-PPIX. Ga-PPIX animal toxicity was determined by injecting 30 final instar *G. mellonella* larvae per group with 5 μ l bolus of 2-fold dilutions of Ga-PPIX ranging from 0.2 mM to 25 mM. After injection, the larvae were incubated at 37°C for 5 days. Every 24 hours, larvae were assessed for death removing dead caterpillars as described previously (4). A dose-response curve shows an effect with increasing concentration, however survival analysis does not show a significant difference between treatment groups and controls, with 3 dead larvae in the 25 mM group compared to a single dead larva in the control group (Fig. 7). Probit analysis estimates the lethal concentration for killing 50% of injected animals (LC₅₀) to be 376 mM Ga-PPIX. This concentration is way beyond the solubility of this compound using an aqueous buffer as well as the concentration range we plan to test based on data published before (8).

Submerged A549 monolayers treated with various concentrations of Ga-PPIX in complete DMEM for 24 h at 37°C with 5% CO₂ were used to test the cell toxicity of this non-ferric metalloporphyrin derivative using the CellTiter-Glo system (Promega, Madison, WI), which directly measures ATP as an indicator of cell viability. This approach showed that Ga-PPIX does not affect cell viability when compared to untreated control as determined by the Kruskal-Wallis test with the Dunn's multiple comparison post-hoc test at concentrations below 320 μ g/ml (Fig. 8). Preliminary studies indicated Ga-PPIX was able to quench luminescence. Considering the absorption spectrum of PPIX, it is not surprising that the signal is diminished with the presence of Ga-PPIX particularly at high concentrations. So, to mitigate the signal reduction, Ga-PPIX containing media was removed, monolayers were washed, and media without Ga-PPIX was placed on cells concomitantly with the application of the CellTiter-Glo reagent. It was noted that monolayers that had been treated with higher Ga-PPIX concentrations (i.e. 640 and 320 μ g/ml) were visibly colored, therefore the differences seen for higher

concentrations may be an artifact of Ga-PPIX remaining in/on A549 cells independent of cell viability. This possibility will receive further attention with assays that do not depend on luminescence.

Taken together, the *G. mellonella* and A549 cell assays showed that Ga-PPIX is not toxic to human cells and an invertebrate host in concentrations that could be within the therapeutic range we plan to test with the animal models proposed in this application.

Interaction with abiotic and biotic surfaces

Motility on semi-solid surfaces

During our work with the ATCC 19606^T, ATCC 17978 and other clinical strains, we observed that *A. baumannii* interacts with semi-solid surfaces by displaying either no motility or two types of motilities: 1) motility on the surface of semi-solid media (0.3% agarose), which we call surface motility; and 2) twitching motility, which occurs on the surface on a Petri dish underneath the 0.3% agarose layer around the inoculation site. We recently reported that production of type IV pili is critical for twitching motility (10), while the cellular mechanisms involved in surface motility remain to be identified and characterized. Since these motility responses are known to play a role in bacterial virulence and not much is known about their biological role in *A. baumannii*, we tested the 29 *A. baumannii* MRSN strains. For this purpose we used 0.3% agarose plates stab-inoculated and incubated overnight at 37°C. Surface motility was recorded by visual inspection of inoculated plates while twitching motility was detected by crystal violet staining of bacteria attached to the surface of the plates after the 0.3% agarose layer was carefully removed. The areas of the surface and twitching motility halos were determined using the program ImageJ (<http://rsb.info.nih.gov/nih-image/>). Table 6 shows that 12 of the 29 *A. baumannii* MRSN strains display surface motility, with strains 4025 and AB5075 being the most and least motile strains, respectively, while the remaining 17 isolates were considered non-motile. Interestingly, none of the tested isolates, including the control strains, displayed a surface motility response similar to that of ATCC 17978, which covered most of the surface of the plate after overnight incubation at 37°C. This study also showed that 18 of the 29 MRSN isolates twitched on the surface of the plate underneath of the agar layer. Further analysis showed that there are no direct correlations between the strain isolation sites and the twitching and/or surface motility phenotypes of the MRSN strains. The same observation was drawn from the analysis of the ATCC 19606^T, ATCC 17978, ACICU and AYE strains, which were used as controls. It is interesting to note that the MRSN strains 2828, 3638, 3806, 4957 and 5001, which are considered representatives of current/modern MDR isolates, and ATCC 19606^T, which is considered an old isolate that does not represent the emergence of *A. baumannii* MDR strains, displayed the same motility phenotype. Taken together, all these observations indicate that the expression of motility is quite variable among *A. baumannii* clinical isolates and independent of time and site of isolation, an observation that parallels the lack of correlation between biofilm formation on plastic and glass surfaces and hydrophobic/hydrophilic cell surface properties (11). Although these are interesting observations that contribute to the overall understanding of the cell biology and pathobiology of *A. baumannii*, they pose a challenge to the use of these functions as alternative targets to treat infections caused by MDR isolates. Nevertheless, we plan to test the virulence role of surface and twitching motility using AB5075 isogenic mutants generated by Dr. C. Manoil.

Interaction with A549 polarized cells

The ability of *A. baumannii* to cause severe infections in hospitalized patients depends not only on its interaction with relevant abiotic surfaces found in medical environments and devices, but also with host cells it targets during colonization and infection. Accordingly, we have been using A549 human alveolar epithelial cells since they are a logical target during the respiratory infections this pathogen causes in compromised hosts (12). More recently, we adapted a polarized system to study host-pathogen interactions since this experimental condition is more representative of liquid/cell-air interfaces found in the lungs than submerged monolayers. Infection of polarized A549 cells with *A. baumannii* ATCC 19606^T has produced very interesting observations we consider relevant to its pathobiology. Thus, we used this system to examine the interaction of AB5075 with this human cell line. Initial experiments have shown that the infection of polarized cells results in a drastic reduction in the surfactant that covers most of the surface of the polarized A549 cells (compare panel A with panels B-C in Fig. 9). We have not observed such a response in similar polarized cell samples infected with either ATCC 19606^T or ATCC 17978 bacteria (data not shown). The micrographs in Fig. 9 also show significant A549 cell damage (panels B-D), the formation of bacterial biofilms on their surfaces (panels C and D) and the presence of long filaments connecting bacteria located on different areas of the polarized sample. Whether these filaments represent bacterial cell appendages, such as pili, or the collapse of exopolysaccharides

present in the biofilm matrix produced by AB5075 bacteria remains to be determined. Taken together, these results provide novel observations on the interaction of AB5075 with human cells that may reflect its higher virulence compared to other *A. baumannii* isolates as reported in the manuscript accepted for publication in mBio (see appendix 4). We plan to use this tissue culture model to test whether the addition of Ga-PPIX has any effect on the host-pathogen interactions revealed by using this experimental approach, which we believe will provide novel insights into the physiology and pathobiology of *A. baumannii*.

Key Research Accomplishments

- Availability of AB5075 insertion mutant libraries that already provided critical mutants to test the role of virulence factors expressed by this MDR isolate.
- Demonstration of the key role the production of acinetobactin and its utilization play in the ability of AB5075 to grow under iron chelation using laboratory experimental conditions.
- Demonstration of the critical role acinetobactin production and utilization play in the virulence of AB5075 using relevant invertebrate (*G. mellonella* larvae) and vertebrate (immunosuppressed mice) experimental infection models.
- Demonstration of the ability of AB5075 to use xenosiderophores under iron chelated conditions, a response that may reflect the outcome of poly-microbial wound infections.
- Detection of variable Ga(NO₃)₃ responses among *A. baumannii* tested strains using laboratory conditions.
- Demonstration of effective anti-bacterial activity of Ga-PPIX against *A. baumannii* isolates independent of culture conditions, media composition and the presence of excess iron.
- Detection of limited sensitivity of *E. coli*, *P. aeruginosa* and *K. pneumoniae* MDR isolates to Ga-PPIX using laboratory conditions.
- Implementation of the *G. mellonella* experimental model as a practical and convenient approach to test the effectiveness of Ga-PPIX and Ga(NO₃)₃ as anti-bacterial agents under relevant *in vivo* conditions.
- Implementation of a tissue culture model that has the potential for providing novel insights into host-pathogen interactions involved in the pathogenesis of severe *A. baumannii* infections and testing antimicrobial agents.

Reportable Outcomes

Presentations

Penwell, W. F., D. L. Zimble, A. C. Beckett, B. A. Arivett, S. E. Fiester, Zurawski, D. V. and L. A. Actis. Variability of virulence factors among *Acinetobacter baumannii* isolates obtained from wounded military personnel. 20th Annual Midwest Microbial Pathogenesis Conference, Columbus, Ohio, September 2013.

Geiger, S. C, B. A. Arivett and L. A. Actis. Determining the antimicrobial mode of action of Ga-PPIX on *Acinetobacter baumannii*. Annual meeting, Ohio Branch American Society for Microbiology, The Ohio State University, Columbus, Ohio, April 2014.

Arivett, B. A., W. F. Penwell, C. Kaufman, R. F. Relich, D. L. Zimble, E. Ohneck, S. E. Fiester and L. A. Actis. Gallium protoporphyrin IX inhibits growth of multidrug resistant *Acinetobacter baumannii*. American Society for Microbiology, 114th General Meeting, Boston, MA, May 2014.

Results regarding the iron uptake phenotype of *A. baumannii* MDRN strains and the effect of iron uptake/metabolism inhibitors were presented and discussed in these meetings and presentations.

Publications

Jacobs, A. C., M. G. Thompson, C. C. Black, J. L. Kessler, L. P. Clark, C. N. McQueary, H. Y. Gancz, B. W. Corey, J. K. Moon, Y. Si, M. T. Owen, J. D. Hallock, Y. I. Kwak, A. Summers, C. Z. Li, D. A. Rasko, **W. F. Penwell**, C. L. Honnold, M. C. Wise, P. E. Waterman, E. P. Lesho, R. L. Stewart, **L. A. Actis**, T. J. Palys, D. W. Craft, and D. V. Zurawski. AB5075, a highly virulent isolate of *Acinetobacter baumannii*, as a model strain for the evaluation of pathogenesis and antimicrobial treatments. Accepted for publication in mBio, 2014.

This manuscript describes the genetic, functional and virulence analysis of *A. baumannii* AB5075, which was selected as a the model MDRN strain to be used in future studies, which will include the analysis of a library of isogenic derivatives generated by transposition mutagenesis with insertions mapped using high-throughput methods.

Arivett, B. A., W. F. Penwell, C. Kaufman, R. F. Relich, D. L. Zimble, S. E. Fiester and L. A. Actis. Gallium protoporphyrin IX inhibits growth of multidrug resistant *Acinetobacter baumannii*. In preparation.

This manuscript, which is based on the presentation we made at the 114th General Meeting of ASM in Boston, MA, is in the final stages of preparation and will be submitted for publication in a peer-reviewed journal sometime this summer.

Conclusions

Because of the generation of *A. baumannii* AB5075 insertion libraries, which were constructed by our collaborators using high-throughput transposon mutagenesis and automated DNA sequencing, we were able to study some critical biological aspects of this strain. Comparative biochemical and functional analyses of the AB5075 wild type parental strain and isogenic insertion derivatives affected in the production of proteins needed for the biosynthesis and transport of siderophores showed that the iron uptake capacity of this strain solely depends on the expression of a fully active acinetobactin-mediated iron acquisition system. This dependency was demonstrated not only under iron-limiting laboratory conditions, but also using *G. mellonella* larvae and immunosuppressed BALB/c mice in experimental infection assays. These results not only validated AB5075 as a proper model strain to study virulence under *in vitro*, *in vivo* and *ex vivo* conditions, but also the critical role iron acquisition plays in the virulence of this strain, which we plan to test using a wound model developed by Dr. Zurawski (13). Equally relevant is the finding that all *A. baumannii* strains isolated from wounded military personnel proved to be sensitive to Ga-PPIX independent of the composition of the media and the presence of free inorganic iron. These observations support our goal of using this anti-microbial agent, which seems to inhibit intracellular iron metabolism rather than acquisition, in the aforementioned experimental infection assays. Such an approach seems feasible not only because of the supporting results obtained with different pathogens (8), but also because Ga-PPIX does not display detectable cell and animal toxicity within the concentration range we plan to test. Although all these observations are encouraging regarding the potential use of Ga-PPIX as an alternative to treat infections caused by MDR *A. baumannii* strains, the efficacy of this non-ferric metalloporphyrin derivative against other wound pathogens is not conclusive and requires some additional studies. Finally, the implementation of a tissue culture model that mimics conditions *A. baumannii* encounters in the human host during respiratory infections has the potential for providing novel and relevant host-pathogen interactions, which could be critical for the infections this pathogen causes in humans and targeting MDR isolates. We will explore the possibility of adapting keratinocyte-based models to examine host-pathogen interactions that are more relevant to cases of wound and skin infections in wounded military personnel as well as civilian patients.

References

1. Dorsey CW, Tomaras AP, Actis LA. 2002. Genetic and phenotypic analysis of *Acinetobacter baumannii* insertion derivatives generated with a Transposome system. *Appl. Environ. Microbiol.* **68**:6353-6360.
2. Dorsey CW, Tomaras AP, Connerly PL, Tolmasky ME, Crosa JH, Actis LA. 2004. The siderophore-mediated iron acquisition systems of *Acinetobacter baumannii* ATCC 19606 and *Vibrio anguillarum* 775 are structurally and functionally related. *Microbiology* **150**:3657-3667.
3. Penwell WF, Arivett BA, Actis LA. 2012. The *Acinetobacter baumannii entA* gene located outside the acinetobactin cluster is critical for siderophore production, iron acquisition and virulence. *PLoS One* **7**:e36493.
4. Gaddy JA, Arivett BA, McConnell MJ, Lopez-Rojas R, Pachon J, Actis LA. 2012. Role of acinetobactin-mediated iron acquisition functions in the interaction of *Acinetobacter baumannii* ATCC 19606^T with human lung epithelial cells, *Galleria mellonella* caterpillars and mice. *Infect. Immun.* **80**:1015-1024.
5. Neres J, Engelhart CA, Drake EJ, Wilson DJ, Fu P, Boshoff HI, Barry CE, 3rd, Gulick AM, Aldrich CC. 2013. Non-nucleoside inhibitors of BasE, an adenylating enzyme in the siderophore biosynthetic pathway of the opportunistic pathogen *Acinetobacter baumannii*. *J. Med. Chem.* **56**:2385-2405.
6. Zimble DL, Penwell WF, Gaddy JA, Menke SM, Tomaras AP, Connerly PL, Actis LA. 2009. Iron acquisition functions expressed by the human pathogen *Acinetobacter baumannii*. *Biometals* **22**:23-32.
7. Stojiljkovic I, Kumar V, Srinivasan N. 1999. Non-iron metalloporphyrins: potent antibacterial compounds that exploit haem/Hb uptake systems of pathogenic bacteria. *Mol. Microbiol.* **31**:429-442.
8. Bozja J, Yi K, Shafer WM, Stojiljkovic I. 2004. Porphyrin-based compounds exert antibacterial action against the sexually transmitted pathogens *Neisseria gonorrhoeae* and *Haemophilus ducreyi*. *Int. J. Antimicrob. Agents* **24**:578-584.
9. McConnell MJ, Actis L, Pachon J. 2013. *Acinetobacter baumannii*: human infections, factors contributing to pathogenesis and animal models. *FEMS Microbiol. Rev.* **37**:130-155.
10. Harding CM, Tracy EN, Carruthers MD, Rather PN, Actis LA, Munson RS, Jr. 2013. *Acinetobacter baumannii* strain M2 produces type IV pili which play a role in natural transformation and twitching motility but not surface-associated motility. *MBio* **4**:e00360-13.
11. McQueary CN, Actis LA. 2011. *Acinetobacter baumannii* biofilms: variations among strains and correlations with other cell properties. *J Microbiol* **49**:243-250.

12. Gaddy JA, Tomaras AP, Actis LA. 2009. The *Acinetobacter baumannii* 19606 OmpA protein plays a role in biofilm formation on abiotic surfaces and the interaction of this pathogen with eukaryotic cells. *Infect. Immun.* **77**:3150-3160.
13. Thompson MG, Black CC, Pavlicek RL, Honnold CL, Wise MC, Alamneh YA, Moon JK, Kessler JL, Si Y, Williams R, Yildirim S, Kirkup BC, Jr., Green RK, Hall ER, Palys TJ, Zurawski DV. 2014. Validation of a novel murine wound model of *Acinetobacter baumannii* infection. *Antimicrob. Agents Chemother.* **58**:1332-1342.

Appendices

Presentation abstracts

- Appendix 1. Penwell, W. F., D. L. Zimbler, A. C. Beckett, B. A. Arivett, S. E. Fiester, Zurawski, D. V. and L. A. Actis. Variability of virulence factors among *Acinetobacter baumannii* isolates obtained from wounded military personnel. 20th Annual Midwest Microbial Pathogenesis Conference, Columbus, Ohio, September 2013.
- Appendix 2. Geiger, S. C, B. A. Arivett and L. A. Actis. Determining the antimicrobial mode of action of Ga-PPIX on *Acinetobacter baumannii*. Annual meeting, Ohio Branch American Society for Microbiology, The Ohio State University, Columbus, Ohio, April 2014.
- Appendix 3. Arivett, B. A., W. F. Penwell, C. Kaufman, R. F. Relich, D. L. Zimbler, S. E. Fiester and L. A. Actis. Gallium protoporphyrin IX inhibits growth of multidrug resistant *Acinetobacter baumannii*. American Society for Microbiology, 114th General Meeting, Boston, MA, May 2014.

Publications

- Appendix 4. Jacobs, A. C., M. G. Thompson, C. C. Black, J. L. Kessler, L. P. Clark, C. N. McQueary, H. Y. Gancz, B. W. Corey, J. K. Moon, Y. Si, M. T. Owen, J. D. Hallock, Y. I. Kwak, A. Summers, C. Z. Li, D. A. Rasko, **W. F. Penwell**, C. L. Honnold, M. C. Wise, P. E. Waterman, E. P. Lesho, R. L. Stewart, **L. A. Actis**, T. J. Palys, D. W. Craft, and D. V. Zurawski. AB5075, a highly virulent isolate of *Acinetobacter baumannii*, as a model strain for the evaluation of pathogenesis and antimicrobial treatments. Accepted for publication in *mBio*, 2014.

Supporting Data Tables

Table 1. WRAIR Gram-negative clinical isolates exhibiting growth and secretion of iron-chelating compounds and catechol.

Species	WRAIR	CAS ^{ac}	Arnow ^{ac}	CAS ^{bc}	Arnow ^{bc}
<i>P. aeruginosa</i>	105777	+/+	+/-	+/+	+/-
	105819	+/+	+/-	+/+	+/-
	105880	+/+	+/-	+/+	+/-
	105857	+/+	+/-	+/+	+/-
	105738	+/+	+/-	+/+	+/-
<i>K. pneumoniae</i>	101436	-/-	-/-	+/+	+/+
	101712	+/+	+/+	+/+	+/+
	105371	-/-	-/-	+/+	+/+
	101488	+/+	+/+	+/+	+/+
	101731	+/+	+/+	+/+	+/+
<i>E. coli</i>	4640	-/-	-/-	+/+	+/+
	105454	+/+	+/+	+/+	+/+
	105547	-/-	-/-	+/+	+/+
	109497	+/+	+/+	+/+	+/+
	108191	+/+	+/+	+/+	+/+
	105433	+/+	+/+	+/+	+/-
	105438	+/+	+/+	+/+	+/+

^aGrown shaking at 200 rpm at 37°C in succinate medium. ^bGrown shaking at 200 rpm at 37°C in M9 minimal medium. ^cTwo parameters were assessed, growth and result of biochemical assay. (+) indicates growth in medium or a positive reaction for each assay. (-) corresponds to no growth or a negative assay result.

Table 2. Siderophore utilization assays.

Strains ^a	BauA ^b	EntA ^c
<i>E. coli</i> 105438	+	+
<i>E. coli</i> 108191	+	+
<i>K. pneumoniae</i> ATCC 13883*	+	+
<i>K. pneumoniae</i> 4640	+	+
<i>K. pneumoniae</i> 101731	+	+
<i>P. aeruginosa</i> PAO1*	-	-
<i>P. aeruginosa</i> 105738	-	-
<i>P. aeruginosa</i> 105857	-	-
<i>A. baumannii</i> ATCC 19606 ^{T*}	-	+

^aStrains used to prepare culture supernatants. ^{b/c}ATCC 19606^T mutants affected in the production of BauA receptor and EntA biosynthetic enzyme, respectively.

*Strains used as controls.

Table 3. Automated MIC of gallium nitrate toward *A. baumannii* strains grown M9 minimal medium containing the synthetic iron chelator 2,2'dipyridyl (DIP).

Strains	Name	Source	Sequenced	Avg 0	Avg 25	Avg 50	Avg 75	Avg 100	Avg 125
406	<i>A. baumannii</i> ATCC 19606 ^T	ATCC	*	0.095	0.051	0.036	0.062	-0.002	-0.004
2488	<i>A. baumannii</i> ATCC 17978	ATCC	*	0.138	0.113	0.074	0.099	0.078	0.128
2620	<i>A. baumannii</i> M2	P. Rather	*	0.086	0.062	0.078	0.080	0.011	0.050
2886	<i>A. baumannii</i> LUH07672	L. Dijkshoorn		0.120	0.082	0.104	0.076	0.051	0.063
2887	<i>A. baumannii</i> LUH08809	L. Dijkshoorn		0.123	0.084	0.061	0.066	0.036	0.057
2888	<i>A. baumannii</i> LUH05875	L. Dijkshoorn		0.149	0.070	0.103	0.084	0.038	0.104
2889	<i>A. baumannii</i> LUH13000	L. Dijkshoorn		0.082	0.067	0.081	0.092	0.047	0.114
2890	<i>A. baumannii</i> RUH00134	L. Dijkshoorn		0.079	0.047	0.060	0.052	0.029	0.026
2891	<i>A. baumannii</i> RUH00875	L. Dijkshoorn		0.069	0.057	0.027	0.015	0.038	0.014
2997	<i>A. baumannii</i> AYE	ATCC	*	0.052	0.067	0.075	0.033	0.080	0.052
2998	<i>A. baumannii</i> SDF	ATCC	*	0.001	0.000	-0.001	0.002	0.118	-0.007
3132	<i>A. baumannii</i> AB967	D. Zurwaski		0.072	0.062	0.084	0.029	0.055	0.040
3133	<i>A. baumannii</i> AB2828	D. Zurwaski		0.143	0.088	0.098	0.058	0.075	0.058
3134	<i>A. baumannii</i> AB3340	D. Zurwaski		0.146	0.072	0.058	0.039	0.069	0.054
3135	<i>A. baumannii</i> AB3560	D. Zurwaski		0.091	0.054	0.040	0.018	0.051	0.045
3136	<i>A. baumannii</i> AB3638	D. Zurwaski		0.043	0.027	0.033	0.010	0.012	0.029
3137	<i>A. baumannii</i> AB3785	D. Zurwaski		0.077	0.054	0.045	0.005	0.058	0.038
3138	<i>A. baumannii</i> AB3806	D. Zurwaski		0.102	0.058	0.003	0.025	0.053	0.053
3139	<i>A. baumannii</i> AB3927	D. Zurwaski		0.061	0.087	0.102	0.019	0.108	0.078
3140	<i>A. baumannii</i> AB4025	D. Zurwaski		0.146	0.063	0.117	0.076	0.077	0.067
3141	<i>A. baumannii</i> AB4026	D. Zurwaski		0.091	0.063	0.068	0.041	0.113	0.053
3142	<i>A. baumannii</i> AB4027	D. Zurwaski		0.150	0.088	0.070	0.009	0.079	0.052
3143	<i>A. baumannii</i> AB4052	D. Zurwaski		0.125	0.072	0.027	0.009	0.061	0.063
3144	<i>A. baumannii</i> AB4269	D. Zurwaski		0.102	0.031	0.031	0.011	0.021	0.026
3145	<i>A. baumannii</i> AB4448	D. Zurwaski		0.077	0.037	0.023	0.019	0.040	0.011
3146	<i>A. baumannii</i> AB4456	D. Zurwaski		0.084	0.049	0.043	0.023	0.075	0.064
3147	<i>A. baumannii</i> AB4490	D. Zurwaski		0.115	0.083	0.151	0.018	0.106	0.050
3148	<i>A. baumannii</i> AB4498	D. Zurwaski		0.153	0.100	0.115	0.068	0.089	0.051
3149	<i>A. baumannii</i> AB4795	D. Zurwaski		0.167	0.088	0.100	0.049	0.103	0.047
3150	<i>A. baumannii</i> AB4857	D. Zurwaski	*	0.122	0.053	0.047	0.017	0.082	0.041
3151	<i>A. baumannii</i> AB4878	D. Zurwaski		0.126	0.049	0.055	0.009	0.075	0.067
3152	<i>A. baumannii</i> AB4932	D. Zurwaski		0.107	0.039	0.018	0.013	0.028	0.018
3153	<i>A. baumannii</i> AB4957	D. Zurwaski		0.054	0.075	0.040	0.013	0.046	0.021
3154	<i>A. baumannii</i> AB4991	D. Zurwaski		0.103	0.056	0.056	0.035	0.056	0.031
3155	<i>A. baumannii</i> AB5001	D. Zurwaski		0.110	0.079	0.110	0.017	0.064	0.045
3156	<i>A. baumannii</i> AB5075	D. Zurwaski	*	0.116	0.086	0.115	0.053	0.103	0.032
3157	<i>A. baumannii</i> AB5197	D. Zurwaski		0.085	0.069	0.093	0.047	0.067	0.027
3158	<i>A. baumannii</i> AB5256	D. Zurwaski	*	0.110	0.077	0.039	0.014	0.062	0.127
3159	<i>A. baumannii</i> AB5674	D. Zurwaski		0.099	0.037	0.049	0.036	0.033	0.057
3160	<i>A. baumannii</i> AB5711	D. Zurwaski	*	0.059	0.034	0.026	0.011	0.026	0.013
3161	<i>A. baumannii</i> ACICU		*	0.136	0.053	0.063	0.031	0.039	0.024

Inocula suspensions were normalized to OD₆₀₀ of 0.2 in M9 minimal medium. One microliter of normalized inoculum was added to 100 µl of M9 minimal medium with 100 µM DIP in 96-well microtiter plates containing varying concentrations of gallium nitrate hydrate (Acros Organics, New Jersey, USA), sealed with AeraSeal microporous sealing film (Phenix Research Products, Ashville, NC, USA) and incubated for 18 h at 37°C. Bacterial growth was then assayed by measuring OD₆₀₀. All liquid handling was performed using a Biomek FX liquid handling instrument with Biomek® software version 3.3.14 (Beckman Coulter,). MICs were determined by OD₆₀₀ on a FilterMax F5 plate reader with Multi-Mode Analysis version 3.4.0.25 (Molecular Devices, Sunnyvale, CA, USA). All experiments were performed twice in triplicate using fresh biological samples each time.

Table 4. Automated MIC of Ga-PPIX toward *A. baumannii* strains grown in cation-adjusted Mueller-Hinton (CAMH) broth containing Ga-PPIX.

Strains	Name	Source	Sequenced	Avg 0	Avg 7.8	Avg 15.6	Avg 31.25	Avg 62.5	Avg 125	Avg 250
406	<i>A. baumannii</i> ATCC 19606 [†]	ATCC	*	0.231	0.264	0.240	0.248	-0.002	0.006	0.003
2488	<i>A. baumannii</i> ATCC 17978	ATCC	*	0.379	0.424	0.420	0.444	0.005	0.011	0.006
2620	<i>A. baumannii</i> M2	P. Rather	*	0.303	0.317	0.141	0.257	-0.002	0.002	0.003
2886	<i>A. baumannii</i> LUH07672	L. Dijkshoorn		0.426	0.309	0.357	0.379	-0.001	0.004	0.006
2887	<i>A. baumannii</i> LUH08809	L. Dijkshoorn		0.493	0.365	0.327	0.339	0.000	0.009	0.022
2888	<i>A. baumannii</i> LUH05875	L. Dijkshoorn		0.328	0.263	0.321	0.329	0.014	0.010	0.004
2889	<i>A. baumannii</i> LUH13000	L. Dijkshoorn		0.407	0.428	0.388	0.363	0.202	0.075	-0.014
2890	<i>A. baumannii</i> RUH00134	L. Dijkshoorn		0.341	0.380	0.394	0.409	0.003	0.005	0.006
2891	<i>A. baumannii</i> RUH00875	L. Dijkshoorn		0.393	0.476	0.520	0.623	0.109	0.012	0.012
2997	<i>A. baumannii</i> AYE	ATCC	*	0.417	0.499	0.522	0.575	0.115	0.003	0.009
2998	<i>A. baumannii</i> SDF	ATCC	*	0.386	0.297	0.252	0.224	0.004	0.013	0.016
3022	<i>A. baumannii</i> A118	M. Tomalsky	*	0.313	0.391	0.375	0.404	-0.001	0.001	-0.001
3132	<i>A. baumannii</i> AB967	D. Zurwaski		0.439	0.505	0.526	0.598	0.023	0.008	0.003
3133	<i>A. baumannii</i> AB2828	D. Zurwaski		0.134	0.160	0.161	0.169	0.002	0.006	0.006
3134	<i>A. baumannii</i> AB3340	D. Zurwaski		0.354	0.409	0.389	0.434	0.003	0.004	0.005
3135	<i>A. baumannii</i> AB3560	D. Zurwaski		0.362	0.411	0.376	0.443	0.001	0.002	0.005
3136	<i>A. baumannii</i> AB3638	D. Zurwaski		0.404	0.425	0.508	0.516	0.000	0.003	0.007
3137	<i>A. baumannii</i> AB3785	D. Zurwaski		0.480	0.511	0.549	0.566	0.003	0.005	0.010
3138	<i>A. baumannii</i> AB3806	D. Zurwaski		0.368	0.406	0.391	0.450	0.009	0.001	0.005
3139	<i>A. baumannii</i> AB3927	D. Zurwaski		0.444	0.512	0.508	0.471	0.001	0.003	0.005
3140	<i>A. baumannii</i> AB4025	D. Zurwaski		0.342	0.344	0.353	0.382	0.044	0.012	0.008
3141	<i>A. baumannii</i> AB4026	D. Zurwaski		0.382	0.417	0.422	0.419	0.013	0.009	0.006
3142	<i>A. baumannii</i> AB4027	D. Zurwaski		0.412	0.371	0.249	0.272	0.023	0.006	0.035
3143	<i>A. baumannii</i> AB4052	D. Zurwaski		0.196	0.379	0.398	0.427	0.002	0.013	0.011
3144	<i>A. baumannii</i> AB4269	D. Zurwaski		0.389	0.409	0.438	0.514	0.002	0.006	0.003
3145	<i>A. baumannii</i> AB4448	D. Zurwaski		0.459	0.556	0.529	0.622	0.011	0.020	0.018
3146	<i>A. baumannii</i> AB4456	D. Zurwaski		0.432	0.570	0.569	0.585	0.005	0.014	0.024
3147	<i>A. baumannii</i> AB4490	D. Zurwaski		0.328	0.378	0.379	0.406	0.063	0.021	0.007
3148	<i>A. baumannii</i> AB4498	D. Zurwaski		0.420	0.473	0.473	0.497	0.001	0.016	0.007
3149	<i>A. baumannii</i> AB4795	D. Zurwaski		0.307	0.403	0.377	0.302	0.003	0.009	0.007
3150	<i>A. baumannii</i> AB4857	D. Zurwaski	*	0.496	0.540	0.498	0.636	0.003	0.025	0.020
3151	<i>A. baumannii</i> AB4878	D. Zurwaski		0.504	0.530	0.550	0.624	0.010	0.023	0.023
3152	<i>A. baumannii</i> AB4932	D. Zurwaski		0.306	0.383	0.393	0.418	0.006	0.010	0.003
3153	<i>A. baumannii</i> AB4957	D. Zurwaski		0.475	0.565	0.518	0.669	0.031	0.067	0.017
3154	<i>A. baumannii</i> AB4991	D. Zurwaski		0.299	0.344	0.348	0.398	0.004	0.004	0.003
3155	<i>A. baumannii</i> AB5001	D. Zurwaski		0.511	0.575	0.414	0.625	0.051	0.013	0.019
3156	<i>A. baumannii</i> AB5075	D. Zurwaski	*	0.467	0.516	0.433	0.619	0.002	0.010	0.009
3157	<i>A. baumannii</i> AB5197	D. Zurwaski		0.415	0.498	0.473	0.526	0.008	0.019	0.007
3158	<i>A. baumannii</i> AB5256	D. Zurwaski	*	0.463	0.533	0.470	0.548	0.079	0.035	0.026
3159	<i>A. baumannii</i> AB5674	D. Zurwaski		0.347	0.405	0.349	0.459	0.003	0.004	0.001
3160	<i>A. baumannii</i> AB5711	D. Zurwaski	*	0.254	0.261	0.156	0.312	0.021	0.013	0.021
3161	<i>A. baumannii</i> ACICU		*	0.357	0.301	0.178	0.205	0.017	0.072	0.004
3284	<i>A. baumannii</i> AB0057			0.358	0.404	0.386	0.445	0.016	0.018	0.001

Inocula suspensions were normalized to OD₆₀₀ of 0.2 in CAMH. One microliter of normalized inoculum was added to 100 μ l of CAMH in 96-well microtiter plates containing varying concentrations of Ga-PPIX (Frontier Scientific, Logan, UT, USA), sealed with AeraSeal microporous sealing film and incubated for 18 h at 37°C. Bacterial growth was then assayed by measuring OD₆₀₀. All liquid handling was performed using a Biomek FX liquid handling instrument with Biomek® software version 3.3.14 (Beckman Coulter,). MICs were determined by OD₆₀₀ on a FilterMax F5 plate reader with Multi-Mode Analysis version 3.4.0.25 (Molecular Devices, Sunnyvale, CA, USA). All experiments were performed twice in triplicate using fresh biological samples each time.

Table 5. Ga-PPIX sensitivity of *E. coli*, *K. pneumoniae* and *P. aeruginosa* MRS isolates.

Species	WRAIR	Sensitivity -LB	Sensitivity - LB+DIP
<i>P. aeruginosa</i>	105777	-	-
	105819	-	-
	105880	-	-
	105857	-	-
	105738	-	-
<i>K. pneumoniae</i>	101436	-	-
	101712	-	-
	105371	-	-
	101488	-	-
	101731	-	-
	4640	-	?
<i>E. coli</i>	105454	-	+
	105547	-	+
	109497	-	+
	108191	-	-
	105433	-	-
	105438	-	+

Sensitivity to Ga-PPIX was determined by disk diffusion assays. Each strain was swabbed onto LB plates with and without 100 μ M DIP. Sterile disks with 50, 20, and 10 μ g Ga-PPIX were applied to the plates. After 24 h incubation at 37°C the zones of inhibition were assessed.

Table 6. Surface and twitching motility of *A. baumannii* MRSN selected isolates and control strains.

Isolates	Isolation site	Surface motility ^a	Area (mm ²)	Twitching motility	Area (mm ²)
967	Blood	-	256.0 ± 24.5	+	2367.9 ± 260
2828	Blood	-	159.9 ± 18.6	-	N/A ^b
3340	Blood	-	154.9 ± 13.2	+	333.6 ± 64.3
3560	Blood	+	613.9 ± 228.1	+	1456.3 ± 728.3
3638	STS ^c	-	181.7 ± 23.5	-	N/A
3785	Blood	+	1862.7 ± 1079.8	-	N/A
3806	STS	-	108.6 ± 9.2	-	N/A
3927	Tibia	+	2338.3 ± 483.3	+	598.1 ± 119.3
4025	Femur	+	9945.4 ± 1476.0	-	N/A
4026	Fibula	+	6788.7 ± 804.5	-	N/A
4027	Femur	+	7480.9 ± 383.9	-	N/A
4052	War wound	-	151.1 ± 9.3	+	1971.1 ± 291.8
4269	War wound	-	119.2 ± 14.7	+	2009.5 ± 415.9
4448	War wound	+	1555.3 ± 745.0	+	1441.2 ± 319.2
4456	Tachasp ^d	+	1151.8 ± 187.5	+	705.9 ± 52.2
4490	War wound	+	547.9 ± 246.8	+	944.9 ± 478.6
4498	Blood	+	8331.5 ± 1103.5	-	N/A
4795	STS-Bone	+	9198.4 ± 273.9	-	N/A
4857	STS-Bone	+	642.8 ± 11.7	+	1058.1 ± 273.5
4878	War wound	-	290.5 ± 51.5	+	2216.5 ± 66.0
4932	Sputum	-	201.7 ± 27.9	+	2102.9 ± 107.8
4957	STS-Bone	-	160.1 ± 9.2	-	N/A
4991	War Wound	+	1012.6 ± 287.8	+	1341.7 ± 76.89
5001	Blood	-	248.6 ± 27.7	-	N/A
5075	Bone	+	521.4 ± 164.3	+	2306.8 ± 57.8
5197	STS	+	687.5 ± 416.8	+	1139.9 ± 175.6
5256	Blood	+	1066.2 ± 270.5	+	1604.4 ± 160.5
5674	Blood	+	544.0 ± 247.9	+	1803.3 ± 227.4
5711	Blood	-	178.8 ± 33.9	+	1823.7 ± 121.2
19606	Urine ^e	-	177.1 ± 13.6	-	N/A
17978	Meningitis ^e	+	18833.2 ± 2987.1	-	N/A
ACICU	Meningitis ^e	-	306.1 ± 71.1	-	N/A
AYE	Urine ^e	+	2210.6 ± 302.3	+	1281.4 ± 360.9

^aSurface motility reflects bacterial motility on the surface of 0.3% agarose plates. Areas smaller than 500 mm² were considered growth around the inoculation site rather true surface motility and therefore classified as motility negative. ^bNot applicable. ^cSevere trauma site. ^dTracheal aspiration. ^eControl strains. (+) and (-)

Figures

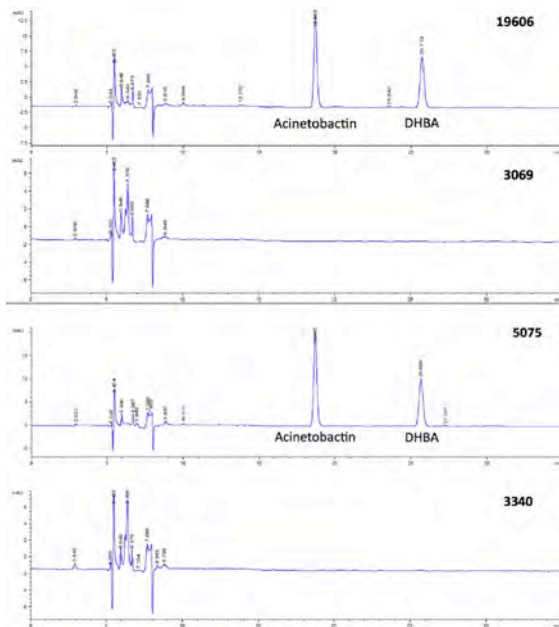


Fig. 1. Detection of acinetobactin and DHBA. M9 culture supernatants of the ATCC 19606^T and AB5075 and their cognate *entA* mutants 3069 and 3340 were analyzed by RP-HPLC.

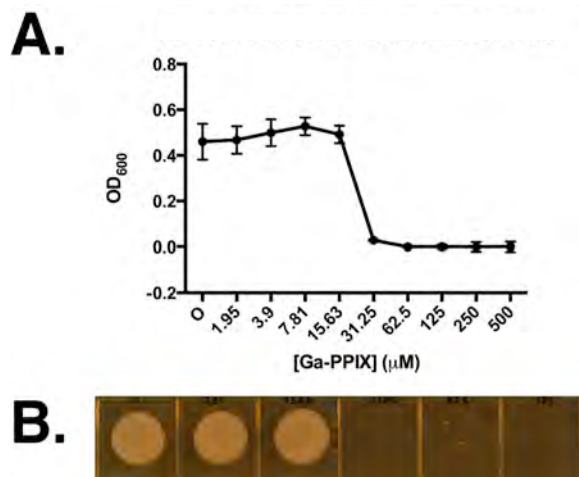


Fig. 3. Susceptibility of the MRSN multi-drug resistant *A. baumannii* AB5075 strain to Ga-PPIX. The MIC of Ga-PPIX was determined by microdilution method in microtiter plates containing MH broth inoculated with 10⁵ AB5075 bacteria (A). B shows MIC with cultures of AB5075 spotted onto MH agar to visualize cell viability that was below spectral detection limits.

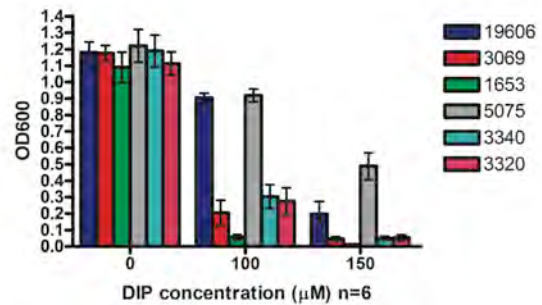


Fig. 2. Bacterial growth under iron-chelated conditions. Growth of cells of the wild-type strain ATCC 19606^T and the isogenic mutants 1653 (*bauA*::Tn) and 3069 (*entA*::Km) was compared with that of the AB5075 parental strain and the isogenic derivatives 3320 (*bauA*::Tn) and 3340 (*entA*::Tn) when cultured in M9 minimal medium containing increasing DIP concentrations.

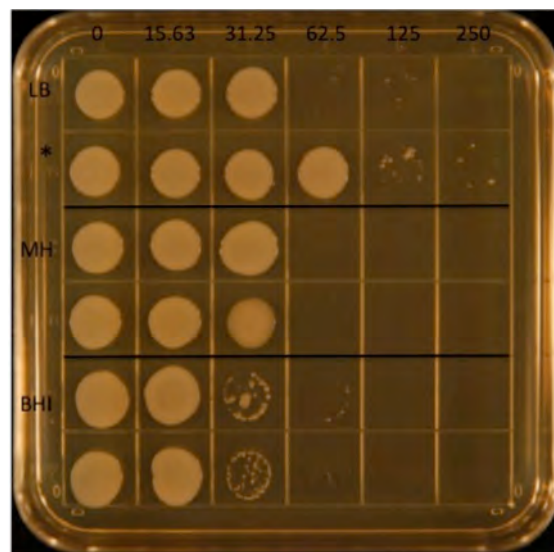


Fig. 4. Effect of Ga-PPIX on *A. baumannii* AB5075 cultured in different media. The Ga-PPIX MIC was tested for Luria Bertani (LB), Mueller-Hinton (MH), and brain heart infusion (BHI). Results were confirmed by plating serial dilutions on LB agar plates containing no antimicrobials and determining colony forming unit (CFU) values. *greater than average growth. Results were recorded after 24 h incubation at 37°C.

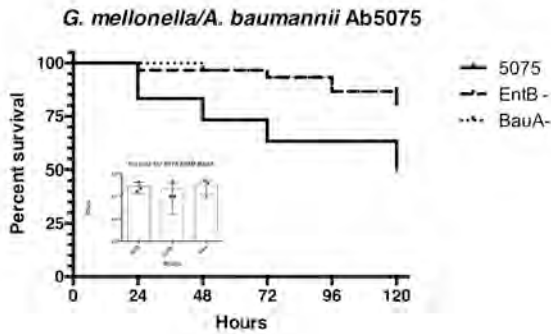


Fig. 5. Kaplan-Meier survival plot of *G. mellonella* larvae injected with AB5075 and derivatives. *G. mellonella* were assayed every 24 h after injection with 10^5 CFU/ml of *A. baumannii* AB5075 or isogenic derivatives *bauA::Tn* (BauA⁻) or *entB::Tn* (EntB⁻) in PBS. Inset shows inocula for each infection. These experiments were done three using fresh biological samples and 10 caterpillars per bacterial strain each time.

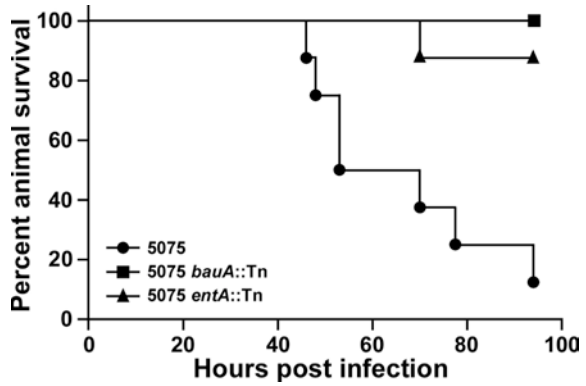


Fig. 6. Kaplan-Meier Survival plot of mice infected with AB5075 and derivatives. Cyclophosphamide-treated mice were intranasally infected with AB 5075 cells (1.4×10^6) or cells of the *bauA::Tn* (1.6×10^6) or *entA::Tn* (1.3×10^6) isogenic derivatives. Animal mortality was scored twice daily for 5 days. Animal experimental procedures were approved by the Institutional Animal Care and Use Committee at WRAIR.

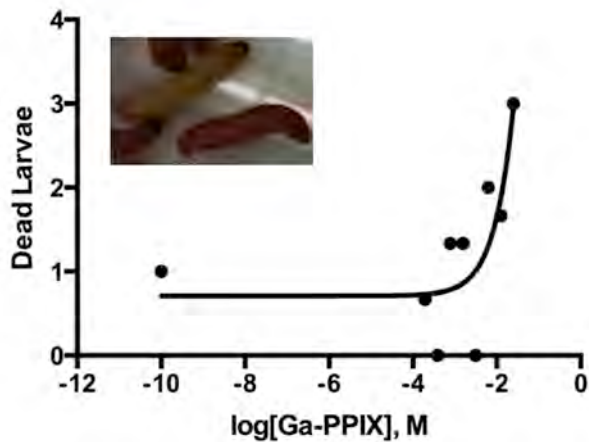


Fig. 7. Nonlinear Log-Dose versus response curve of Ga-PPIX in *G. mellonella*. The larvae were injected $5 \mu\text{l}$ with varying concentrations of Ga-PPIX solubilized in PBS containing 0.5 N NaOH and 15% DMSO, and then followed for survival over 5 days. Total death was plotted against survival. Inset shows a normal white colored larva that had not been injected and three pink larvae that had been injected with $5 \mu\text{l}$ of 25 mM Ga-PPIX.

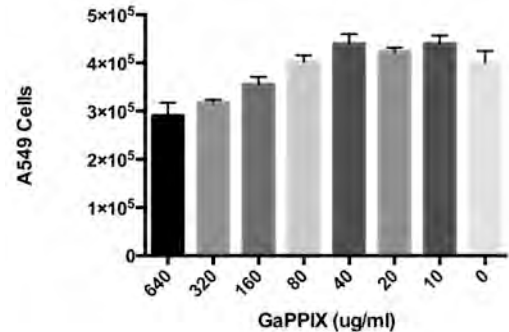


Fig. 8. A549 cell viability after exposure to Ga-PPIX. Submerged A549 monolayers were treated with various concentrations of Ga-PPIX in complete DMEM for 24 h at 37°C with 5% CO_2 . A549 viability was assessed using CellTiter-Glo. A549 cell count was interpolated from known concentrations of viable A549 cells. Experiments were done twice in duplicate using fresh samples each time.

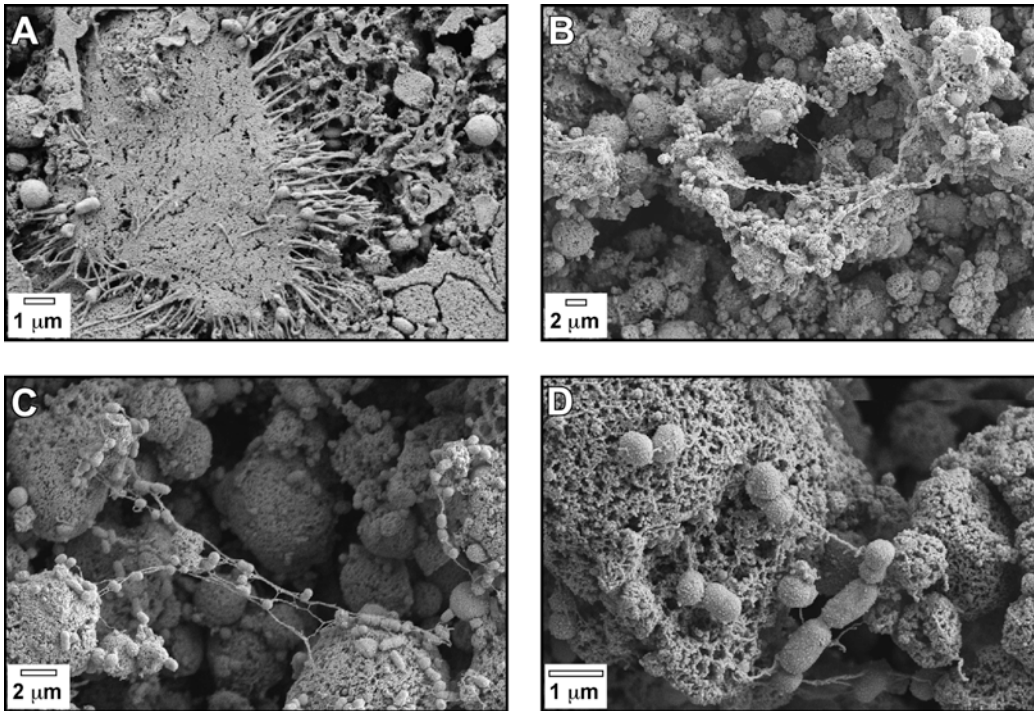
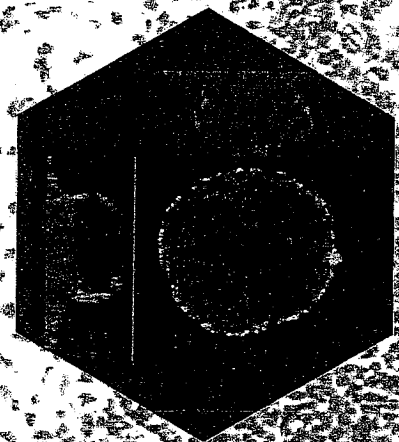
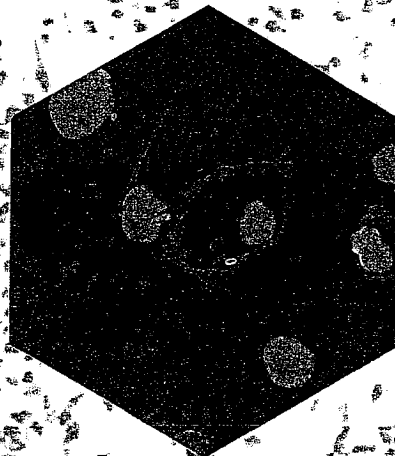
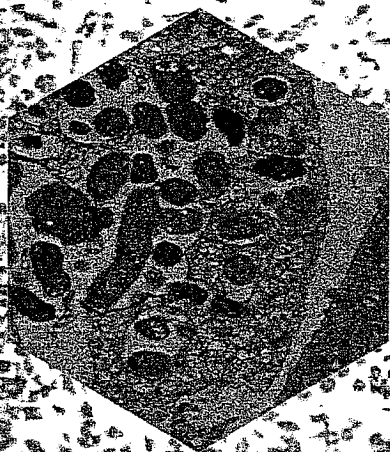


Fig. 9. Interaction of *A. baumannii* AB5075 with polarized A549 human alveolar epithelial cells. A549 alveolar epithelial cells were polarized on trans-well membrane plates and infected with bacteria for 72 hours (panels B-D). Non-infected cells were used as a control (panel A). The samples were dehydrated, prepared for and analyzed using scanning electron microscopy.

20th

Annual Midwest Microbial Pathogenesis Conference



Wexner Medical Center



NATIONWIDE CHILDREN'S
When your child needs a hospital, everything matters.™

44. VARIABILITY OF VIRULENCE FACTORS AMONG *ACINETOBACTER BAUMANNII* ISOLATES OBTAINED FROM WOUNDED MILITARY PERSONNEL

Penwell, W.F.¹, Zimbler, D.L.¹, Beckett, A.C.¹, Richards, A. M.¹, Arivett, B. A.¹, Fiester, S.E.¹, Zurawski, D.V.², Actis, L.A.¹

¹Department of Microbiology, Miami University, Oxford, OH

²Department of Wound Infections, Walter Reed Army Institute of Research, Silver Spring, MD

Acinetobacter baumannii is a Gram-negative, nosocomial human pathogen that causes a broad range of infections, which include pneumonia, urinary tract, blood and skin infections. Many studies have focused on the antibiotic resistance of this opportunistic pathogen, but information regarding potential virulence factors is lagging. Our study investigates virulence-related phenotypes from a diverse set of twenty-nine *A. baumannii* clinical isolates obtained from the Walter Reed Army Institute of Research (WRAIR) that were isolated from wounded military personnel from 2006 to 2010. The ability of these strains to grow under iron-limiting conditions on LB agar supplemented with the synthetic iron chelator 2, 2'-dipyridyl (DIP), as well as the production of siderophores using biochemical, cross-feeding assays and HPLC analyses were examined. The ability of these strains to form biofilm on either plastic or glass was determined by growing the strains in LB broth supplemented with or without DIP. Isolates were also inoculated onto motility agar and examined for their ability to display surface and/or twitching motility. Because iron acquisition is a key aspect of *A. baumannii* virulence, the effect of Gallium-protoporphyrin IX (Ga-PPIX) on the growth of *A. baumannii* strains cultured on LB agar plates was included in this study as a potential therapeutic. While the results from this work indicate variations among different *A. baumannii* clinical isolates in regard to their capacity to grow under iron-limiting conditions, produce siderophores, form biofilm on abiotic surfaces and display motility, all tested strains are sensitive to Ga-PPIX. Together, the results from these studies indicate a variation in the expression of virulence traits when comparing different *A. baumannii* isolates, which create challenges in developing new therapeutic agents. However, all strains tested display sensitivity to Ga-PPIX, which could be used as a therapeutic agent for *A. baumannii*-infected individuals.

**Annual Meeting
Ohio Branch of the American
Society for Microbiology**



The Ohio State University

**Dorothy M. Davis Heart & Lung Research
Institute and Biomedical Research Tower
Columbus, OH**

April 11-12, 2014



THE OHIO STATE UNIVERSITY

**Official Meeting Program
and
Conference Abstracts**

Determining the Antimicrobial Mode of Action of GaPPIX on *Acinetobacter baumannii*

Sarah C. Geiger*, Brock A. Arivett, and Luis A. Actis
Miami University

Acinetobacter baumannii is a multi-drug resistant, Gram-negative, opportunistic nosocomial pathogen that is a serious threat worthy of immediate attention. This pathogen is recognized for its robust biofilm formation in various hospital environments and its capacity to resist a wide range of antibiotics and antimicrobials some of which, such as ethanol, serve as a carbon source and enhance its virulence. *A. baumannii* is also the causative agent for many infections, resulting in diagnoses including severe pneumonia and necrotizing fasciitis. To address the need for alternative therapeutics for multi-drug resistant *A. baumannii* isolates, this research investigates the sensitivity of this pathogen to gallium protoporphyrin IX (GaPPIX), a compound that exploits this organism's use of heme-iron. Iron is imperative for the microorganism's growth, and because GaPPIX has a similar molecular structure to heme, it may be acquired and transported by heme-related systems that remain to be characterized in this pathogen. Since GaPPIX does not have the same chemical properties as heme, it initiates bacterial death by another unknown mechanism. GaPPIX resistant derivatives of the ATCC 19606 type strain and 5075 strain were isolated using GaPPIX. The genome of these two resistant isolates will be sequenced with the objective of understanding the mechanisms by which GaPPIX enters the bacterial cell and affects its antimicrobial activity. These studies should provide novel insights into the pathobiology of *A. baumannii* and the potential use of GaPPIX as an effective antimicrobial agent to treat infections caused by multi-drug resistant strains.

Appendix 3

FINAL PROGRAM

asm2014



American Society for Microbiology
114th General Meeting
May 17–20, 2014
Boston, Massachusetts

www.asm.org/asm2014



AMERICAN
SOCIETY FOR
MICROBIOLOGY

- 501 Seroprevalence, Molecular Detection and Risk Factors Associated with Bovine Brucellosis in Pakistan**
S. Ali¹, H. Neubauer², F. Melzer², I. Khan³, Q. Ali⁴, E. N. Abatih⁵, N. Ullah¹, M. W. Akbar³, S. Akhter¹; ¹Pir Mehr Ali Shah Arid Agriculture Univ., Rawalpindi, Pakistan, ²Friedrich-Loeffler-Inst., Germany, Jena, Germany, ³Univ. of Vet. and Animal Sci., Lahore, Pakistan, ⁴Natl. Vet. Lab., Islamabad, Pakistan, ⁵Inst. of Tropical Med., Antwerpen, Belgium
- 502 Detection and Investigation of Pasteurellosis in Bovine Animals in the Lori Province, Armenia**
A. Abrahamyan; State Food Safety Services, Armenia
- 503 African Swine Fever Detection, Investigation, and Control during an Outbreak in the Noyemberyan Province of Armenia**
A. Melikyan; State Food Safety Services, Armenia
- 504 Occurrence of Bovine Tuberculosis in Cattle Farms in Zaria and Kaduna and Possible Transmission Through Milk**
P. N. Mbianga, V. J. Umoh, A. I. O, K. C. A; Ahmadu Bello Univ., Zaria, Nigeria

Sunday, May 18

12:30 p.m. – 1:45 p.m.

038 Antimicrobial Susceptibility II (Division A)

12:30 p.m. – 1:45 p.m. | Exhibit Hall B

- 505 Effects of Green Tea Polyphenols on Endospore Germination in *Bacillus cereus*, *B. megaterium*, and *B. subtilis***
N. Laskar¹, H. Tahir¹, T-C. Chu², L. H. Lee¹; ¹Montclair State Univ., Montclair, NJ, ²Seton Hall Univ., South Orange, NJ
- 506 Gallium Protoporphyrin IX Inhibits Growth of Multidrug-Resistant *Acinetobacter baumannii***
B. A. Arivett¹, W. F. Penwell¹, C. M. Kaufman², R. F. Relich³, S. E. Fiester¹, L. A. Actis¹; ¹Miami Univ., Oxford, OH, ²IU Hlth. Pathology Lab., Indianapolis, IN, ³IU Sch. of Med., Indianapolis, IN
- 507 Efflux Pump Inhibitors Overcome Antimicrobial Resistance to Berberine**
S. Arcidiacono¹, J. Soares¹, S. Sarangapani²; ¹U.S. Army Natick RD&E Ctr., Natick, MA, ²ICET Inc., Norwood, MA
- 508 Nisin Susceptibility of *Staphylococcus aureus* Biofilms**
F. G. Santos^{1,2}, B. Pitts², P. S. Stewart^{2,3}, H. C. Mantovani¹; ¹Univ. Federal de Viçosa, Viçosa - MG, Brazil, ²Ctr. for Biofilm Engineering, Montana State Univ., Bozeman, MT, ³Montana State Univ., Bozeman, MT
- 509 Antimicrobial Susceptibility and Time-Kill Analysis of Single and Combined Essential Oil Blends against Clinical and Non-Clinical Isolates of Bacteria and Fungi**
E. C. Adukwu¹, V. Edwards-Jones²; ¹Univ. of the West of England, Bristol, United Kingdom, ²Manchester Metropolitan Univ., Manchester, United Kingdom
- 510 Characterization of *Staphylococcus aureus* Isolates from Ear Discharges of Outpatients of Hospitals and Clinics: Antimicrobial Susceptibility Profile and Distribution of CA-MRSA Isolates**
N. Yoshida¹, T. Ikematsu², H. Sunose³, K. Hayasaki⁴, K. Hirano⁵, H. Iida⁶, A. Kanayama¹, I. Kobayashi¹; ¹Toho Univ., Tokyo, Japan, ²Kashiwa Ikematsu ENT Clin., Chiba, Japan, ³Tokyo Women's Med. Coll. of East Med. Ctr., Tokyo, Japan, ⁴Narashino Daiichi Hosp., Chiba, Japan, ⁵Mildis Pediatrics and ENT Clin., Tokyo, Japan, ⁶Toride Ikematsu ENT Clin., Ibaraki, Japan
- 511 Antimicrobial Profile of Essential Oils Extracted from Wild versus Cultivated *Origanum ehrenbergii* against Enteric Bacteria**
T. A. Kumosani¹, E. K. Barbour¹, S. K. Dankar², H. A. Shaib¹, E. I. Azhar¹, A. P. Iyer¹, S. M. Harakeh¹; ¹King Abdulaziz Univ., Jeddah, Saudi Arabia, ²American Univ. of Beirut, Beirut, Lebanon

- 512 Food Borne Pathogenic Bacteria Inhibition Using Silver Nanoparticles**
K. Vig¹, C. Bell¹, B. Crenshaw¹, M. Miller², S. Pillai¹, S. R. Singh¹; ¹Alabama State Univ., Montgomery, AL, ²Auburn Univ., Auburn, AL
- 513 MDRevealer: A New Software Program to Accelerate the Identification Multi-, Extensively, and Pan-Drug Resistant Bacteria**
R. J. Clifford, R. S. Clifford, P. E. Waterman, E. P. Lesho; Walter Reed Army Inst. of Res., Silver Spring, MD
- 039 Biofilm Biology and Pathogenesis II (Division B)**
12:30 p.m. – 1:45 p.m. | Exhibit Hall B
- 514 The Role of O-Antigen and Capsule-Like Complex (CLC) in *Francisella tularensis* Biofilm Formation and Matrix Composition**
A. E. Champion, A. Bandara, T. J. Inzana; Virginia Tech, Blacksburg, VA
- 515 The Interactive Metabolome of Polymicrobial Communities**
V. Phelan, P. Dorrestein; Univ. of California, San Diego, La Jolla, CA
- 516 Biofilm Formation by Avian Pathogenic *Escherichia coli***
R. M. Ramirez, M-X. Haro, P. Miranda, S-H. Sánchez, L-E. Vidales; Univ. Autónoma de Zacatecas, Zacatecas, Mexico
- 517 Propionibacteria Acnes Recovered from Atherosclerotic Arteries Undergo Biofilm Dispersion in Response to Increased Levels of Norepinephrine.**
B. B. Lanter, D. G. Davies; Binghamton Univ., Binghamton, NY
- 518 Population Dynamics and Genetic Recombination in Multi-Serotype *Streptococcus pneumoniae* Biofilms on Human Pharyngeal Cells**
J. E. Vidal, S. Chochua, F. Sakai, N. T. Jacobs, S. Chancey, D. S. Stephens, K. P. Klugman; Emory Univ., Atlanta, GA
- 519 nagZ Triggers Gonococcal Biofilm Disassembly**
S. Bhoopalan¹, A. Piekarowicz¹, J. P. Dillard², J. D. Lenz², D. C. Stein¹; ¹Univ. of Maryland, College Park, MD, ²Univ. of Wisconsin-Madison, Madison, WI
- 520 Thermal Augmentation of Vancomycin against Staphylococcal Biofilms**
R. Sturtevant, L. Pavlovsky, M. Solomon, J. Younger; Univ. of Michigan, Ann Arbor, MI
- 521 Precise Regulation of the Genes Encoding Contact-Dependent Growth Inhibition (CDI) System Proteins during Burkholderia Biofilm Formation**
E. C. Garcia, P. A. Cotter; Univ. of North Carolina at Chapel Hill, Chapel Hill, NC
- 522 Characterization of the BfmRS Two-Component Regulatory System in *Acinetobacter* Clinical Strains**
E. J. Ohneck¹, S. E. Fiester¹, D. L. Zimble¹, P. N. Rather², L. A. Actis¹; ¹Miami Univ., Oxford, OH, ²Emory Univ. Sch. of Med., Atlanta, GA
- 523 Intrinsic Expression of Insulin Receptors on *Staphylococcus aureus***
B. J. Plotkin, C. Wasson, S. Halkyard; Midwestern Univ., Downers Grove, IL
- 524 Role of DNA Binding Protein in Stabilizing the Edna in *S. epidermidis* Biofilm**
P. Sharma, M. Ganesan, M. J. Solomon, J. G. Younger; Univ. of Michigan, Ann Arbor, MI
- 525 Pleiotropic Effects of Cigarette Smoke on the Virulence of *Staphylococcus aureus***
R. Kulkarni¹, I. Subudhi¹, S. Antala², F. E. Amaral², A. J. Ratner², S. Jeyaseelan¹; ¹Louisiana State Univ., Baton Rouge, LA, ²Columbia Univ., New York, NY

Gallium Protoporphyrin IX inhibits growth of Multidrug Resistant *Acinetobacter baumannii*

Brock A. Arivett^{1*}, William F. Penwell¹, Cynthia Kaufman², Ryan F. Relich³, Daniel L. Zimble¹, Emily Ohneck¹, Steven E. Fiester¹, and Luis A. Actis¹

Department of Microbiology, Miami University, Oxford, OH 45056, USA¹

Division of Clinical Microbiology, IU Health Pathology Laboratory, Indianapolis, IN 46202²

Department of Pathology and Laboratory Medicine, IU School of Medicine, Indianapolis, IN 46202³

Introduction: The opportunistic human pathogen *Acinetobacter baumannii* is prevalent in hospitals and some strains have acquired extensive antibiotic resistance (MDR). So, new therapeutics must be found. The non-reducible ferric iron analogue gallium nitrate has been shown to effectively inhibit growth and treat infections *in vitro* and *in vivo*; although its inhibitory effects require iron-limiting conditions that induce the expression of active iron-acquisition systems. Previous studies have shown that *A. baumannii* utilize heme as an iron source and some strains, such as SDF, only use heme-iron. These findings prompted our study of gallium protoporphyrin IX (Ga-PPIX), a metal containing heme-derivative, which is lethal to *Neisseria gonorrhoeae*, as a therapeutic for MDR *A. baumannii* isolates.

Methods: Strains were routinely cultured for three passages on 5% sheep red blood cell agar followed by growth in cation-adjusted Mueller-Hinton broth. Ga-PPIX solubility was determined by octanol partitioning. Toxicity and therapy was assayed with *Galleria mellonella*. Isolates were confirmed by MALDI-TOF MS using a Bruker microflex analyzer and MALDI Biotyper v3.1 software. Doxycycline susceptibility was carried out by the Kirby-Bauer method according to standard procedures. The Epsilometer test (Etest®)-based MIC, VITEK® 2 XL and the BD Phoenix were used according to the manufacturer's instructions. Interpretive criteria were based on CLSI breakpoints, with the exception of the gentamicin MIC for isolate *A. baumannii* 19606^T; EUCAST breakpoints were used.

Results: In this study, Ga-PPIX inhibited the growth of 39 *A. baumannii* strains and exhibited low toxicity toward *G. mellonella*. Ga-PPIX partitioned into the organic layer, but exhibited fast killing kinetics *in vitro*. Ga-PPIX increased survival of experimentally infected *G. mellonella*.

Conclusions: Ga-PPIX is effective against MDR *A. baumannii* isolates. In spite of Ga-PPIX's poor solubility, its ability to inhibit growth of all tested strains is sufficient to warrant further investigations as an antimicrobial for MDR organisms. The low toxicity and ability to treat experimental infections increase the attractiveness of this compound. However, derivatization of Ga-PPIX to increase its water solubility may make this derivate a more effective antimicrobial agent.

AB5075, a Highly Virulent Isolate of *Acinetobacter baumannii*, as a Model Strain for the Evaluation of Pathogenesis and Antimicrobial Treatments

AQ: au Anna C. Jacobs,^a Mitchell G. Thompson,^a Chad C. Black,^a Jennifer L. Kessler,^a Lily P. Clark,^a Christin N. McQueary,^a Hanan Y. Gancz,^a Jay K. Moon,^a Yuanzheng Si,^a Matthew T. Owen,^b Justin D. Hallock,^b Yoon I. Kwak,^c Amy Summers,^a Charles Z. Li,^a David A. Rasko,^d William F. Penwell,^e Cary L. Honnold,^f Matthew C. Wise,^f Paige E. Waterman,^c Emil P. Lesho,^c Rena L. Stewart,^b Luis A. Actis,^e Thomas J. Palys,^a David W. Craft,^a Daniel V. Zurawski^a

AQ: aff Department of Wound Infections, Walter Reed Army Institute of Research, Silver Spring, Maryland, USA^a; Division of Orthopaedics, University of Alabama at Birmingham, Birmingham, Alabama, USA^b; Multidrug-resistant Organism and Surveillance Network, Walter Reed Army Institute of Research, Silver Spring, Maryland, USA^c; Institute for Genome Sciences, University of Maryland School of Medicine, Baltimore, Maryland, USA^d; Department of Microbiology, Miami University, Oxford, Ohio, USA^e; Department of Pathology, Walter Reed Army Institute of Research, Silver Spring, Maryland, USA^f

D.W.C. and D.V.Z. contributed equally to this article.

ABSTRACT *Acinetobacter baumannii* is recognized as an emerging bacterial pathogen because of traits such as prolonged survival in a desiccated state, effective nosocomial transmission, and an inherent ability to acquire antibiotic resistance genes. A pressing need in the field of *A. baumannii* research is a suitable model strain that is representative of current clinical isolates, is highly virulent in established animal models, and can be genetically manipulated. To identify a suitable strain, a genetically diverse set of recent U.S. military clinical isolates was assessed. Pulsed-field gel electrophoresis and multiplex PCR determined the genetic diversity of 33 *A. baumannii* isolates. Subsequently, five representative isolates were tested in murine pulmonary and *Galleria mellonella* models of infection. Infections with one strain, AB5075, were considerably more severe in both animal models than those with other isolates, as there was a significant decrease in survival rates. AB5075 also caused osteomyelitis in a rat open fracture model, while another isolate did not. Additionally, a Tn5 transposon library was successfully generated in AB5075, and the insertion of exogenous genes into the AB5075 chromosome via Tn7 was completed, suggesting that this isolate may be genetically amenable for research purposes. Finally, proof-of-concept experiments with the antibiotic rifampin showed that this strain can be used in animal models to assess therapies under numerous parameters, including survival rates and lung bacterial burden. We propose that AB5075 can serve as a model strain for *A. baumannii* pathogenesis due to its relatively recent isolation, multidrug resistance, reproducible virulence in animal models, and genetic tractability.

IMPORTANCE The incidence of *A. baumannii* infections has increased over the last decade, and unfortunately, so has antibiotic resistance in this bacterial species. *A. baumannii* is now responsible for more than 10% of all hospital-acquired infections in the United States and has a >50% mortality rate in patients with sepsis and pneumonia. Most research on the pathogenicity of *A. baumannii* focused on isolates that are not truly representative of current multidrug-resistant strains isolated from patients. After screening of a panel of isolates in different *in vitro* and *in vivo* assays, the strain AB5075 was selected as more suitable for research because of its antibiotic resistance profile and increased virulence in animal models. Moreover, AB5075 is susceptible to tetracycline and hygromycin, which makes it amenable to genetic manipulation. Taken together, these traits make AB5075 a good candidate for use in studying virulence and pathogenicity of this species and testing novel antimicrobials.

Received 27 March 2014 Accepted 10 April 2014 Published XXX

Citation Jacobs AC, Thompson MG, Black CC, Kessler JL, Clark LP, McQueary CN, Gancz HY, Moon JK, Si Y, Owen MT, Hallock JD, Kwak YI, Summers A, Li CZ, Rasko DA, Penwell WF, Honnold CL, Wise MC, Waterman PE, Lesho EP, Stewart RL, Actis LA, Palys TJ, Craft DW, Zurawski DV. 2014. AB5075, a highly virulent isolate of *Acinetobacter baumannii*, as a model strain for the evaluation of pathogenesis and antimicrobial treatments. mBio 5(3):e01076-14. doi:10.1128/mBio.01076-14.

Editor Howard Shuman, University of Chicago

Copyright © 2014 Jacobs et al. This is an open-access article distributed under the terms of the [Creative Commons Attribution-Noncommercial-ShareAlike 3.0 Unported license](https://creativecommons.org/licenses/by-nc-sa/4.0/), which permits unrestricted noncommercial use, distribution, and reproduction in any medium, provided the original author and source are credited.

Address correspondence to Daniel V. Zurawski, daniel.v.zurawski.ctr@mail.mil.

AQ: A *Acinetobacter baumannii* is an opportunistic, Gram-negative pathogen that thrives in clinical settings and is often multidrug resistant (MDR), factors which earn it a place among the ESKAPE (*Enterococcus faecium*, *Staphylococcus aureus*, *Klebsiella pneumoniae*, *Acinetobacter baumannii*, *Pseudomonas aeruginosa*, and *Enterobacter* species) pathogens of clinical importance (1). Some recent isolates are resistant to all typically used antibiotics

except colistin and tigecycline and thus are called extensively or extremely drug-resistant (XDR) *A. baumannii* (2). MDR/XDR *A. baumannii* strains are a worldwide problem for clinicians and caregivers in the hospital setting, particularly in the intensive care unit (ICU) (3). *A. baumannii* is also often isolated from infections of severe wounds sustained in military combat. These infections are responsible for increased morbidity, with prolonged wound

healing and amputations of extremities when limbs cannot be salvaged (4, 5). *A. baumannii* was a predominant isolate from wounded soldiers serving in Iraq (4, 5) and was associated with wartime polytrauma injuries in the past (6). Additionally, there may be a link between *A. baumannii* and crush injuries, as *A. baumannii* infections were also prevalent after the recent large earthquakes in Haiti (7) and China (8).

Another disturbing development that has increased the clinical importance of *A. baumannii* infections is that many strains have become highly antibiotic resistant. For example, in previous decades, *A. baumannii* isolates obtained from both military and civilian settings were often carbapenem sensitive. Now, the majority of U.S. military isolates are carbapenem resistant (9). This trend has also been mirrored in civilian hospitals around the world (10). Recently, even colistin-resistant strains have emerged in the military health care system (11). The latter development is deeply troubling, as colistin is considered the last line of defense against these MDR isolates. Exacerbating this problem is the lack of new treatments in the pharmaceutical pipeline (12); therefore, research on *A. baumannii* virulence factors is urgently needed, as they could constitute potentially novel targets for future antimicrobials.

While previous studies attempted to examine the virulence of different clinical *A. baumannii* strains utilizing *in vivo* model systems (13, 14), the majority of *A. baumannii* researchers still use two American Type Culture Collection (ATCC) strains, ATCC 19606^T and ATCC 17978, which were isolated more than 50 years ago and are not significantly antibiotic resistant. These strains are certainly more amenable to genetic manipulation than most clinical isolates (15, 16) and share considerable genome homology (>90%) to current *A. baumannii* isolates (17), but they are not representative of contemporary isolates of this rapidly evolving pathogen. Some researchers, recognizing that the ATCC isolates are dated, have performed studies with more recent clinical isolates; however, genetic manipulation of such isolates has depended on susceptibility to aminoglycosides (18–20), which is often not found in clinical strains (21). Therefore, our goal was to carry out a systematic study of our own contemporary clinical strains isolated from patients in the U.S. military health care system to identify a strain that is more representative of current clinical isolates, that is highly virulent in established model infections, and that can be genetically manipulated without a potential sacrifice with respect to virulence and antibiotic resistance. Not only does identifying such a strain account for more recent clinical outcomes, but the increased virulence in animal models allows greater statistical power in screening new therapeutics. Moreover, the ability to manipulate the genome allows the study of virulence factors, some of which may be responsible for the emergence of this pathogen in more recent years.

RESULTS

Defining genetic characteristics of *A. baumannii* isolates. In order to identify potential reference strains, a diverse set of 33 *A. baumannii* isolates was chosen based on genetic, isolation site, and antibiotic resistance differences from more than 200 *A. baumannii* strains isolated between 2004 and 2010 from patients in the U.S. military health care system. AB0057, first isolated in 2004 at Walter Reed Army Medical Center, was also included as a comparator because this strain is well characterized, and its genome was previously sequenced (22).

The diversity set of *A. baumannii* isolates was determined via pulsed-field gel electrophoresis (PFGE) analysis and a multiplex PCR assay previously developed to identify the international clonal complexes (ICC). Separately, antibiograms were determined using two different automated bacterial identification systems. The majority of strains were found to be multidrug resistant, typical of current clinical strains (see Table S1 in the supplemental material). As shown in Fig. 1, the genetic similarity of the strains, as determined by PFGE, ranged from 45 to 100%. PFGE types were considered to represent the same clones when their genetic similarity was >80% (23); based on this cutoff, the 33 strains represent 19 unique clones. When the genetic relatedness of these 19 clones was compared, it was found that the majority of them clustered into three groups, which generally aligned with the ICC designations determined by multiplex PCR (Fig. 1 and Table 1) (24). Exceptions were the isolates AB3560, AB4456, and AB4857, which were determined to be ICC III by the multiplex assay but appeared to be ICC I via PFGE. In this case, we relied on the multiplex data (Table 1) to be definitive. These data were used to select four representative strains for genome sequencing and evaluation in animal models.

Three of the strains chosen each represented one of the three ICC groups, AB5075 (ICC I), AB5711 (ICC II), and AB4857 (ICC III). The fourth strain, AB5256 was an outlier, as the OXA-51 allele from this strain was amplified with group I primers (24), while the *csuE* allele was not. The isolates were sequenced (25) and compared to previously sequenced *A. baumannii* genomes using the BLAST score ratio (BSR) approach (26). This method compares putative peptides encoded in each genome based on the ratio of BLAST scores to determine if they are conserved (BSR value \geq 0.8), divergent ($0.8 >$ BSR $>$ 0.4), or unique (BSR $<$ 0.4). The majority of the proteomes were similar among strains, meaning they had a BSR of $>$ 0.4; however, each isolate also had a set of unique proteins (see Table S2 in the supplemental material). These results are similar to what has been found previously with MDR *A. baumannii* clinical isolates (17), suggesting that the strains used in this study are not genetic outliers.

Virulence assessed in the *Galleria mellonella* model. Strains were first tested in a *Galleria mellonella* infection model, as this model is well established to assess virulence and novel therapeutics for bacterial pathogens, including *A. baumannii* (27, 28). *G. mellonella* larvae were infected with an approximate dose of 1.0×10^5 CFU with each of the four sequenced *A. baumannii* isolates, AB4857, AB5075, AB5256, and AB5711, as well as control strain AB0057. Worms were observed for 6 days, and death was recorded. Within 24 h postinfection, approximately 25% of AB5075-infected worms remained, while the other four strains had survival rates of 70% or higher (Fig. 2). By the end of the 6-day study, AB5075-infected worms had a survival rate of 16%; strains AB4857 and AB5256 were considered moderately pathogenic in this model, with survival rates of 50% and 35%, respectively. The least lethal strains were AB5711 and AB0057, with survival rates of 85% and 83%, respectively. Phosphate-buffered saline (PBS)-injected control worms displayed 100% survival through the course of the study. Based on these data, it was hypothesized that AB5075 was more virulent than the other four strains tested. Using the Mantel-Cox test with Bonferroni correction for multiple comparisons, Kaplan-Meier curves were compared, and AB5075 was found statistically to be more lethal than AB4857, AB5711, and AB0057 (all *P* values $<$ 0.0125). While AB5256 had a higher

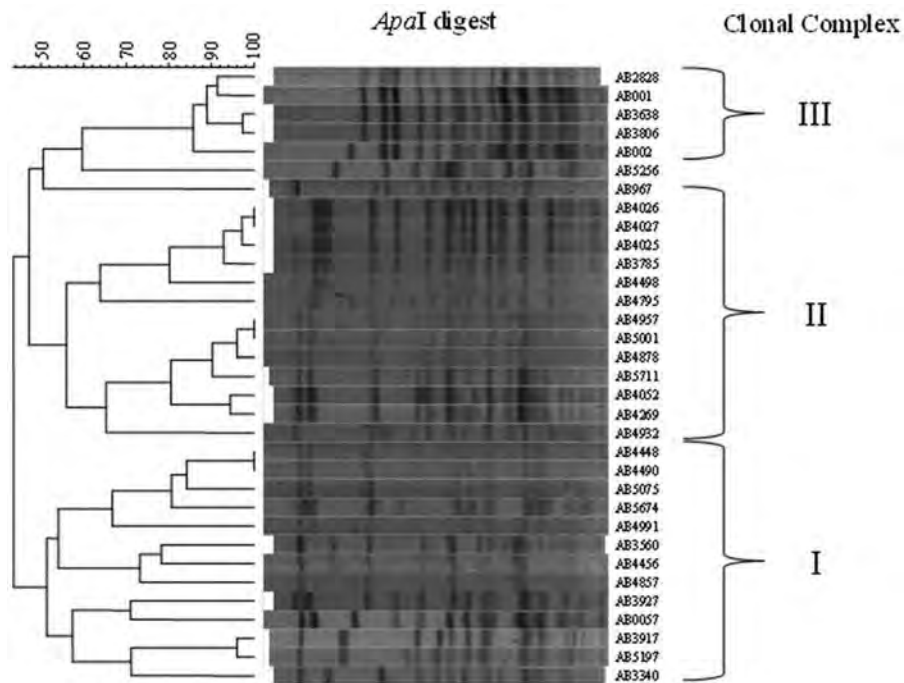


FIG 1 Pulsed-field gel electrophoresis of *A. baumannii* strains. Genomic DNA was isolated from 33 *A. baumannii* clinical isolates, digested with *ApaI*, and separated by pulsed-field gel electrophoresis (PFGE). Patterns of electrophoresis were compared using BioNumerics 6.0 software. The ICC was determined by multiplex PCR analysis, and brackets delineate the approximate grouping of each strain.

survival rate in this study than AB5075, the difference was not significant after the Bonferroni correction.

Separately, to compare the lethality of AB5075 to that of more commonly utilized *A. baumannii* model strains, the 50% lethal doses (LD_{50}) of AB5075, ATCC 17978, and ATCC 19606^T were determined in *G. mellonella*. The LD_{50} of AB5075 was 1.0×10^4 CFU. In contrast, the LD_{50} of ATCC 17978 and ATCC 19606^T were 5.0×10^5 and 1.0×10^6 , respectively.

Virulence assessed in the mouse pulmonary model. *A. baumannii* strains were examined in a murine pulmonary model of infection, because this model is commonly used to assess bacterial virulence and drug efficacy, and survival can be assessed rapidly after an inoculum is delivered (14, 29). The animals were immunocompromised with two doses of cyclophosphamide before inoculation, a treatment that allows *A. baumannii* to establish an infection (14). Mice were inoculated on day 0 with one of the five representative *A. baumannii* strains at a dose of 5.0×10^6 CFU and monitored for 6 days. Consistently, mice infected with AB5075 had a mortality rate of 70% within 48 to 72 h and a 6-day survival rate of 25% (Fig. 3). The other four strains tested, AB0057, AB5711, AB5256, and AB4857, were less lethal than AB5075 in this model, with 6-day survival rates of 65, 80, 80, and 85%, respectively. The log-rank (Mantel-Cox) test with Bonferroni correction determined that AB5075 time-to-death results were statistically significant compared to the other clinical isolates ($P < 0.0125$). The clinical scores of each infected animal also correlated with the survival plots; AB5075-infected mice displayed more severe illness than mice infected with the other strains. In a separate experiment, mice inoculated with 5.0×10^6 cells of ATCC 17978 or ATCC 19606^T resulted in minimal clinical scores and no animal death (data not shown).

Lung bacterial burden in these infections was assessed on days 2 and 3, at the height of illness. The lung CFU/g values for the five infecting strains were compared using a Kruskal-Wallis test followed by a Dunn's multiple comparison test. On day 2, the lungs of AB5256-infected mice had significantly less *A. baumannii* than AB4857-, AB0057-, and AB5075-infected lungs ($P \leq 0.05$) but not AB5711-infected lungs. On day 3, AB5256 displayed a significant decrease in CFU/g compared only to AB5075 (Fig. 4). The four other strains assessed in the model had no significant difference in lung bacterial burden, with the median log CFU/g ranging from 8.5 to 9.3 on day 2 and 8.0 to 8.9 on day 3.

Development of genetic tools in an *A. baumannii* model strain. Our success in establishing AB5075 infections in multiple animal models suggests that the isolate would be an attractive model strain for studying *A. baumannii* virulence. However, in addition to an ideal model strain's being highly virulent in animal models, the ability to genetically manipulate the isolate is vital for the study of *A. baumannii* pathogenicity. Because antibiotic resistance determinants are central to many types of genetic manipulations, such as transposon mutagenesis, the antibiotic sensitivity profile of AB5075 was examined in detail. It was observed that AB5075 is susceptible to tetracycline, doxycycline, and related antibiotics (see Table S1 in the supplemental material) and to high levels of erythromycin and hygromycin.

With these known susceptibilities in mind, a method previously developed in *A. baumannii* (30) was adapted for creating AB5075 isogenic mutants by utilizing the *hph* gene, encoding hygromycin resistance, from pMQ300 (31) and the EZ Tn5 (Epicentre Biotechnologies, Madison, WI) to develop a Tn5-based mutagenesis system. This system was used to generate a library of ~6,700 transposon mutants. DNA sequencing of the library was

TABLE 1 *A. baumannii* strains used in this study^a

Strain	MRSN	Isolation site	Yr isolated	Clonal complex ^b	Source
AB001	1332	ND	ND	ND	C. Murray
AB002	1333	ND	ND	ND	C. Murray
AB0057	1311	Blood/sepsis	2004	I	This study
AB967	1308	Blood/sepsis	2003	III	This study
AB2828	846	Blood/sepsis	2006	III	This study
AB3340	847	Blood/sepsis	2006	I	This study
AB3560	848	Blood/sepsis	2006	III	This study
AB3638	849	Posterior wound	2007	III	This study
AB3785	853	Blood/sepsis	2007	II	This study
AB3806	854	Leg wound	2007	III	This study
AB3917	1309	Blood/sepsis	2007	ND	This study
AB3927	856	Tibia/osteomyelitis	2007	I	This study
AB4025	858	Femur/osteomyelitis	2007	II	This study
AB4026	859	Fibula/osteomyelitis	2007	II	This study
AB4027	860	Femur/osteomyelitis	2007	II	This study
AB4052	863	War wound	2007	II	This study
AB4269	877	War wound	2007	II	This study
AB4448	899	War wound	2007	I	This study
AB4456	903	Tracheal aspirate	2007	III	This study
AB4490	906	War wound	2008	I	This study
AB4498	907	Blood	2008	II	This study
AB4795	930	Bone/osteomyelitis	2008	II	This study
AB4857	939	Ischial/osteomyelitis	2008	III	This study
AB4878	941	War wound	2008	II	This study
AB4932	949	Sputum	2008	II	This study
AB4957	951	Sacral/osteomyelitis	2008	II	This study
AB4991	953	War wound	2008	I	This study
AB5001	954	Blood/sepsis	2008	II	This study
AB5075	959	Tibia/osteomyelitis	2008	I	This study
AB5197	960	STS/tissue	2008	I	This study
AB5256	961	Blood/sepsis	2009	NA	This study
AB5674	963	Blood/sepsis	2009	I	This study
AB5711	1310	Blood/sepsis	2009	II	This study
ATCC 19606 ^T	NA	Urine	1948	ND	ATCC
ATCC 17978	NA	Spinal meningitis	1951	ND	ATCC
RUH134	NA	Urine	1982	II	L. Dijkshoorn
RUH875	NA	Urine	1984	I	L. Dijkshoorn
RUH5875	NA	Unknown, Netherlands	1997	III	L. Dijkshoorn
ACICU	NA	Outbreak isolate, Rome, Italy	2005	II	M. Tolmasky

AQ: B ^a MRSN, ●●●●; ND, no data; NA, not applicable; STS, sterile swab site (most likely from an infected wound).

^b As determined by multiplex assay performed in this study. AB5256 was considered NA because only the OXA-51 amplicon was amplified from group 1 primer set (31).

performed as previously described (32), yielding 2,548 unique transposon insertions and 68.5% coverage of the genome.

As a further means of modifying the genome, the same hygromycin cassette was inserted into the pUC18T-mini-Tn7T-Zeo vector, and this vector was introduced via conjugation into AB5075. Tn7 insertion into the chromosome was selected for by growth on 250 µg/ml hygromycin and confirmed by PCR across the *attTn7* site on the 3' end of the *glmS* gene in the AB5075 chromosome. As proof of concept for the use of Tn7 for gene insertion in the chromosome, the *lux* operon was inserted into the *attTn7* site. This resulted in bioluminescence of this strain, and subsequent subculturing of AB5075::Tn7-*lux* over 7 days without antibiotic selection did not affect the bioluminescent signal (see Fig. S1A in the supplemental material), suggesting that the Tn7 insertion in the chromosome is stable. Additionally, when this strain was cultured in LB broth, there was no growth defect compared to the wild-type isolate AB5075 (see Fig. S1B in the supplemental material). These methods provide us with a means of interrupting and inserting genes on the chromosome, both of which are essential in studying bacterial pathogenesis.

Evaluation of rifampin as proof of concept. As a proof of concept for the use of AB5075 as a model strain for assessing novel antimicrobials, rifampin treatment against AB5075 was tested in the *G. mellonella* and murine pulmonary models. In *G. mellonella*, 30 min after worms were inoculated with 6.0×10^5 CFU of AB5075, they received a treatment injection of 5 or 10 mg/kg rifampin. By 41 h postinfection, all worms infected with AB5075 and receiving PBS treatment had died (Fig. 5). Conversely, worms treated with 5 or 10 mg/kg rifampin had survival rates of 94 and 100%, respectively, at this time point. At the end of the 4-day study, survival rates were 50 and 78%, respectively. The Mantel-Cox test determined that the time to death for AB5075-infected worms was statistically reduced compared to that for rifampin-treated worms ($P < 0.001$).

To further assess AB5075 as a model strain, the mouse lung model was used to examine the efficacy of rifampin. Mice infected intranasally with 5.0×10^6 CFU of AB5075 were treated once daily intraperitoneally (IP) with 2.5, 5, or 10 mg/kg rifampin, and survival was monitored for 48 h. At time of death, or euthanasia at 48 h postinfection, lungs were collected to determine bacterial

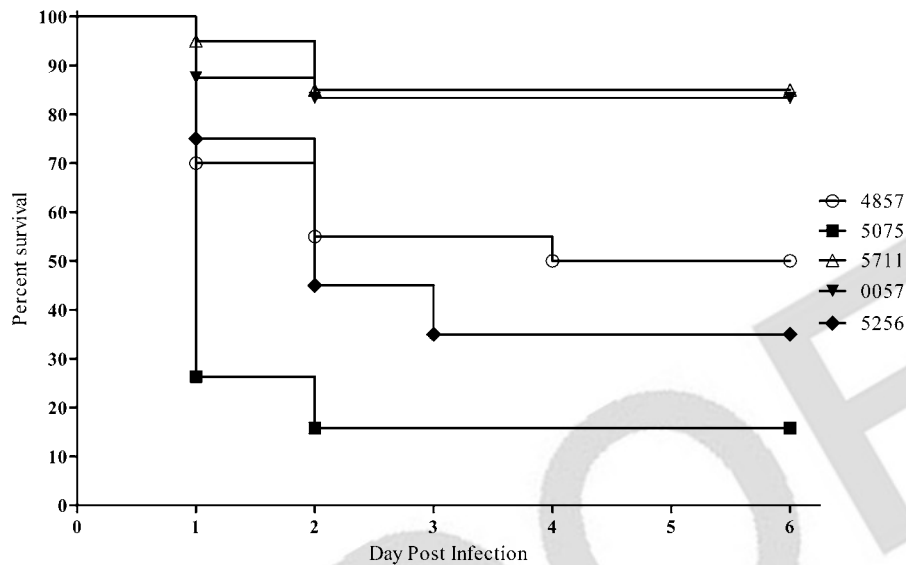


FIG 2 Survival of *Galleria mellonella* larvae infected with *A. baumannii*. Kaplan-Meier survival curves of *G. mellonella* infected with 1.0×10^5 CFU of selected strains of *A. baumannii* are shown. Curves were compared via the Mantel-Cox test with the Bonferroni correction for multiple comparisons. AB5075 showed significantly increased mortality compared to AB4857, AB5711, and AB0057 ($P < 0.0125$).

F6 load. As shown in Fig. 6A, at 48 h after inoculation, only 12.5% of mice infected but not treated with rifampin survived, whereas infected mice receiving 5 and 10 mg/kg rifampin had survival rates of 87.5 and 100%, respectively. These differences in survival were found by the Mantel-Cox test to be statistically significant ($P = 0.0035$ and 0.0008 , respectively) compared with mice infected but not treated with rifampin. Mice treated with 2.5 mg/kg rifampin had a 48-h survival rate of 20%, which was not statistically different from that of the control group.

The levels (CFU/g) of bacteria in lung tissue correlated with the survival curves. The median levels in the control and 2.5 mg/kg-

treated groups were almost identical, at 9.04 and 9.07 log CFU/g, respectively. Figure 6B shows a decrease in the median log CFU/g for mice treated with 5 and 10 mg/kg rifampin, with values of 8.10 and 4.86, respectively. The Kruskal-Wallis test, followed by Dunn's multiple comparison test, found a statistically significant difference in bacterial burden when the control group was compared to animals treated with 5 or 10 mg/kg rifampin ($P < 0.05$).

DISCUSSION

The goal of the work presented in this report was to identify a model strain of *A. baumannii* that represented current infection

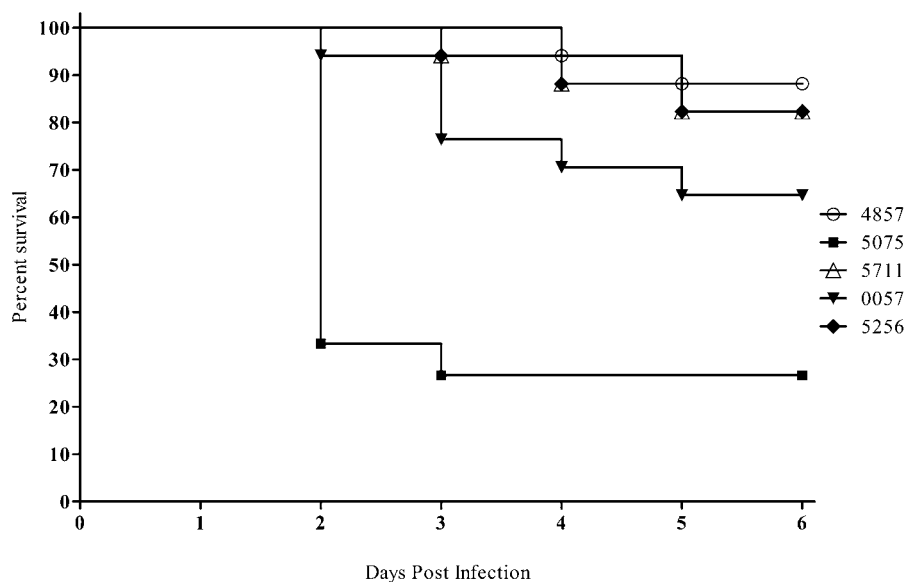


FIG 3 Assessment of *A. baumannii* virulence with the mouse pulmonary model. Kaplan-Meier survival curves of mice infected with 5.0×10^6 CFU of selected *A. baumannii* strains. Curves were compared via the Mantel-Cox test with the Bonferroni correction for multiple comparisons. AB5075 showed significantly increased mortality compared to AB4857, AB5711, AB0057, and AB5256 ($P < 0.0125$).

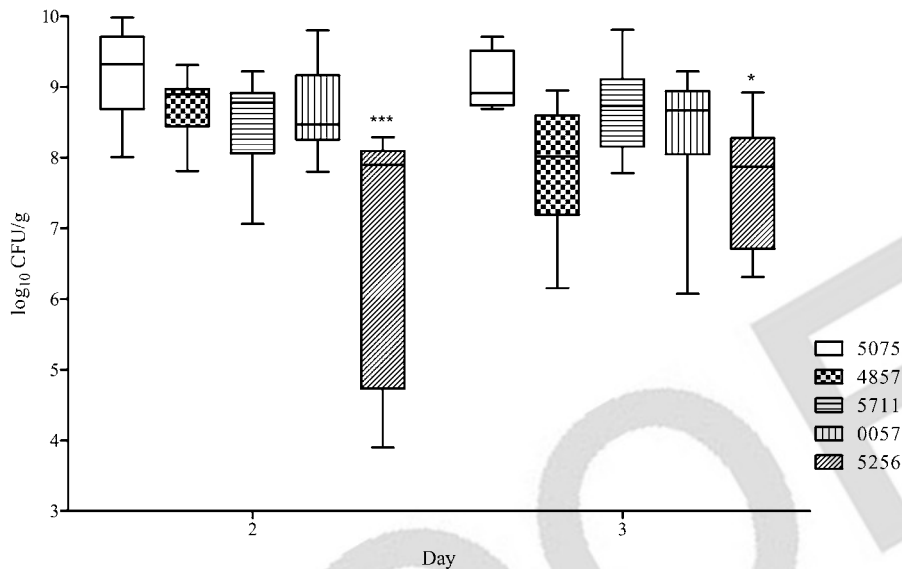


FIG 4 Bacterial levels in lung tissue in the mouse pulmonary model. Box-and-whisker plots of CFU burdens in lungs are shown for days 2 and 3 postinfection. Boxes show median and interquartile ranges, while whiskers represent the 95% confidence interval CI. Strains were compared via the Kruskal-Wallis test followed by Dunn's multiple comparisons posttests. * and ***, $P < 0.05$ and 0.001 , respectively.

isolates, was highly virulent in multiple animal models, and was amenable to genetic manipulation. A strain fitting these characteristics would be clinically relevant and could be utilized in various models to study novel therapeutics, and the ability to create isogenic mutants would be critical in investigating genes required for virulence and the pathogenesis of severe infections in the human host. In our comprehensive studies of isolates representative of each major clonal complex group, we identified one such strain, AB5075.

Previous studies compared the virulence of *A. baumannii* strains in single infection models, including a murine pulmonary model (13, 14) and a *G. mellonella* model (33). Other work also compared the virulence of a single strain, ATCC 19606^T, in multiple models *in vivo* (34); however, to our knowledge, this is the first study that used several infection models in parallel to compare multiple strains using representative isolates from each clonal group. Importantly, when we compared infections caused by other *A. baumannii* strains, including the widely used ATCC

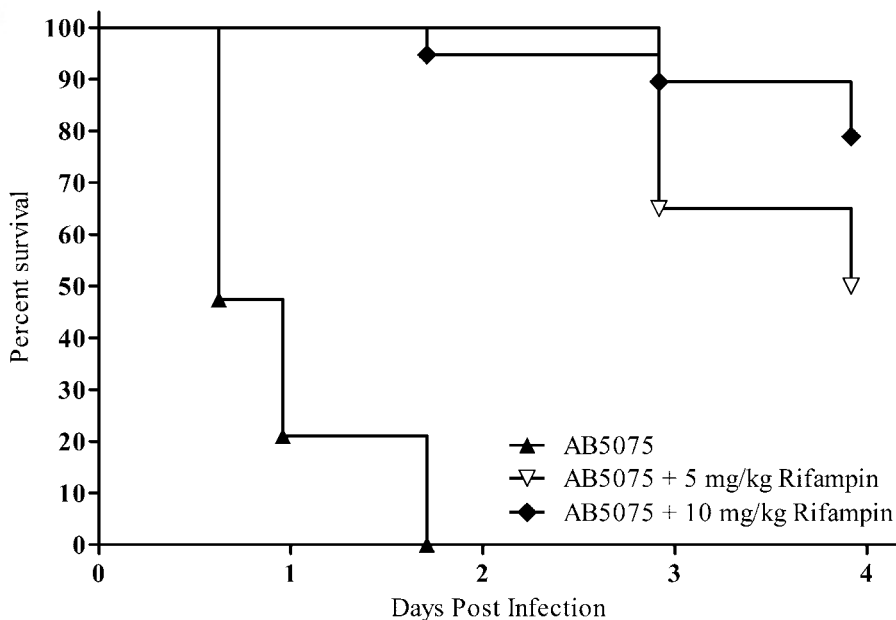


FIG 5 Rifampin as proof of concept in the *G. mellonella* model. Kaplan-Meier survival curves of *G. mellonella* infected with 6.0×10^5 CFU of AB5075 are shown. Worms received a single treatment, 30 min postinfection, of DMSO, 5 mg/kg rifampin, or 10 mg/kg rifampin. Curves were compared via the Mantel-Cox test. The control-treated worms showed significantly increased mortality compared to rifampin-treated worms ($P < 0.001$).

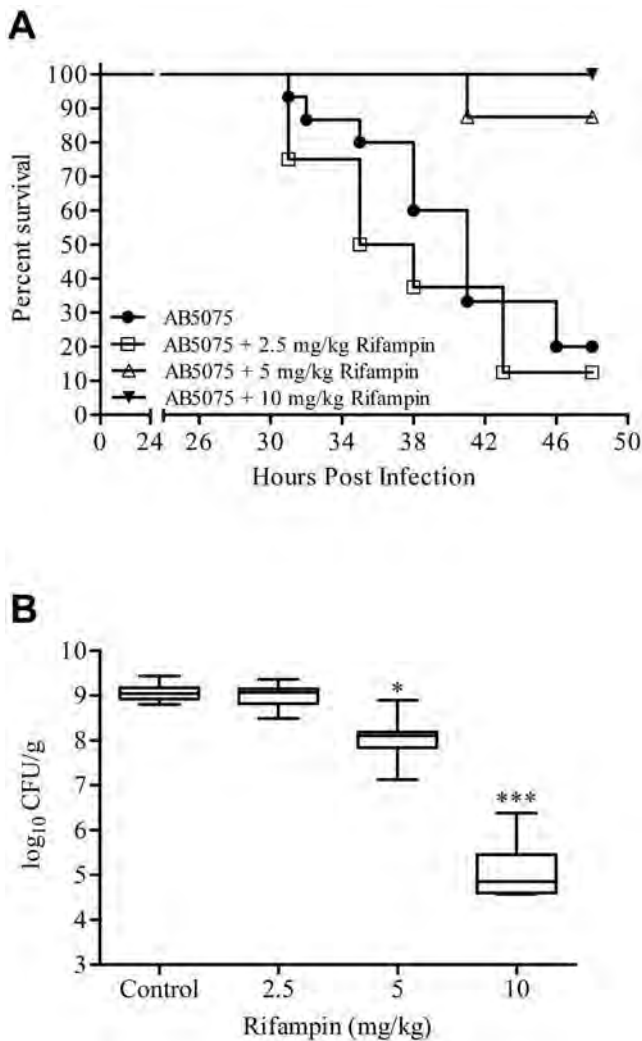


FIG 6 Rifampin as proof of concept in the mouse lung model. (A) Kaplan-Meier survival curves of mice infected with 5.0×10^6 CFU of selected strains of *A. baumannii* are shown. Mice were treated once daily IP with 0, 2.5, 5, or 10 mg/kg rifampin. Curves were compared via the Mantel-Cox test. Rifampin treatments of 5 and 10 mg/kg resulted in significantly increased survival compared to the untreated control ($P = 0.0035$ and 0.0008 , respectively). (B) Box-and-whisker plots of CFU burdens within lungs are shown for day 2 postinfection. Boxes show median and interquartile ranges, while whiskers represent 95% CI. Treatments were compared via the Kruskal-Wallis test followed by Dunn's multiple comparisons posttests. * and ***, $P < 0.05$ and 0.001 , respectively.

19606^T and ATCC 17978, we did not observe the same severe infection as was consistently observed with AB5075.

In the *G. mellonella* and mouse pneumonia models, AB5075 infection resulted in survival rates consistently below 25%, providing a wide spectrum between infected and uninfected animals to assess novel therapies or genetically mutated strains. Additionally, in the mouse pulmonary model, blood samples and lung histopathology from AB5075-infected mice were consistently positive for the presence of *A. baumannii* (data not shown) and, combined with the high lung bacterial burden observed, offer further means of evaluation in this model. Furthermore, while a recent publication claimed that *A. baumannii* could not cause osteomyelitis in a rat fracture model (35), our data showed that

AB5075 could establish an infection in this model and that *A. baumannii* could still be cultured from the bone after 28 days postinfection (see the supplemental material). Recently, we also successfully developed a murine wound model of infection with AB5075, using a small inoculating dose (36). Therefore, the use of AB5075 in additional animal models further demonstrates the great utility of AB5075, as it can serve as a model strain for a variety of studies. The increased virulence of AB5075 in these models also results in larger differences between infected and uninfected animals compared to other tested strains, which allows for less ambiguous results, high statistical power, and thus a requirement for fewer animals to obtain publishable data.

In addition to the successful use of AB5075 in animal models, we were able to exploit the susceptibility of AB5075 to hygromycin to generate a Tn5 transposon insertion library and use a Tn7 transposon derivative to insert genes into the genome of this strain. In collaboration with the Manoil laboratory at the University of Washington, we were able to sequence the Tn5 transposon library using a convenient high-throughput sequencing method. Further, C. Manoil and his team illustrated the genetic utility of AB5075 by generating a Tn5 insertion library utilizing a tetracycline-based transposon system (C. Manoil, ●●●●●, unpublished results). It is expected that these sequenced transposon insertion libraries will be powerful tools for future investigations, as similar libraries have been utilized with success with other bacterial pathogens (37, 38). In the future, the Manoil laboratory will distribute wild-type and mutant derivatives of AB5075 (<http://www.gs.washington.edu/labs/manoil/baumannii.htm>). AQ: D

The ability to interrupt or mutate specific genes via transposon insertion and complement mutations via Tn7-mediated chromosomal insertion provides a powerful toolkit to answer important questions, such as the nature of specific genes and gene products that are critical for virulence in the host. We believe that AB5075, and the genetic tools and animal models we have designed around this strain, will serve as a platform to readily and reproducibly test mutants in putative virulence factor genes and assess novel antimicrobials. Moreover, we encourage other research groups to use AB5075 as a model strain and to take advantage of the tools we are developing to test their own hypotheses about virulence determinants of *A. baumannii*.

MATERIALS AND METHODS

Bacterial strains, growth media, and clinical microbiology. All work was carried out under biosafety level II or II+ conditions. All the *A. baumannii* strains used in this study can be found in Table 1. Routine growth and strain maintenance was carried out in Luria-Bertani Lennox (LB) broth and agar. Bacterial identification, antibiograms, and MIC were determined using the Vitek 2 (bioMérieux, France) and Phoenix (Becton, Dickinson and Co., Franklin Lakes, NJ) automated systems according to the manufacturer's instructions. Rifampin was obtained from Sigma-Aldrich (St. Louis, MO), prepared in dimethyl sulfoxide (DMSO), and then further diluted in sterile saline.

Pulsed-field gel electrophoresis. The pellet from an overnight broth culture was resuspended in 2 ml 10 mM Tris-HCl, 10 mM EDTA (pH 8.0) to a density equivalent to 0.5 McFarland. Suspensions were mixed with equal volumes of melted 1.6% SeaKem Gold agarose (Lonza, Walkersville, MD), dispensed into wells of a plug mold, and allowed to solidify. The plugs were incubated for 2 h in 20 mg/ml proteinase K and cell lysis buffer (50 mM Tris-HCl, 50 mM EDTA [pH 8.0], 1% *N*-lauroylsarcosine, sodium salt) at 54°C. Subsequently, the plugs were washed four times in TE buffer (10 mM Tris-HCl, 10 mM EDTA [pH 8.0]) and then incubated in a digestion buffer consisting of 50 U of ApaI restriction enzyme, NEBuffer

4, and bovine serum albumin (New England BioLabs, Ipswich, MA) at 25°C for at least 2 h. Electrophoresis was performed at a constant voltage of 200 V by the CHEF-DR II system (Bio-Rad Laboratories, Hercules, CA) with pulse times ramping from 7 to 20 s for 18.5 h. Gels were stained with ethidium bromide and photographed under UV light. PFGE clustering was determined by using the unweighted-pair group method with arithmetic averages (UPGMA) and Dice's coefficient (BioNumerics version 6.0, created by Applied Maths NV).

Multiplex PCR assay. Multiplex PCR methods were followed directly from the work of Turton et al. (24), with modified reaction volume and reagents. Briefly, *A. baumannii* templates were prepared from a single colony grown on Luria-Bertani (LB) agar and resuspended in Lyse and Go PCR reagent according to the manufacturer's instructions (Thermo Scientific, Rockford, IL). PCRs were prepared in 20- μ l volume using DreamTaq master mix (Thermo Scientific).

Genome sequencing and bioinformatic analysis. Genome analysis was performed as previously described (17), with AB5075, AB5711, AB4857, and AB5256 included in the bioinformatic comparisons. Unique genes were determined using the BLAST score ratio analysis (26). BLAST score ratio (BSR) is an *in silico* approach to conduct comparative proteomic analyses based on proteins predicted to be encoded in a genome (26). BSR was used to compare the proteins encoded in the newly sequenced strains with three isolates from the University of Maryland (17) and eight previously sequenced reference isolates (SDF, AYE, ATCC 17978, ADP1, AB0057, ATCC 19606^T, ACICU, and AB307). The BSRs were calculated as the ratio of raw BLASTP score for the query to the raw BLASTP score of the reference strain. BSR cutoffs of ≥ 0.8 , < 0.8 to > 0.4 , and < 0.4 were used to determine whether a gene is conserved, divergent, or unique, respectively. A BSR value of 0.8 corresponds to ~85 to 90% identity over 90% of the length of a protein sequence, indicating a highly conserved sequence, while a BSR value of 0.4 corresponds to 30% identity over 30% of the length of a protein sequence, indicating a unique sequence (26).

Galleria mellonella infection model. *A. baumannii* strains were grown overnight in an orbital shaker (37°C, 200 rpm), and overnight cultures were then diluted 100-fold into fresh medium and grown for 3 h. Cells were collected by centrifugation (5 min, 5,000 \times g), washed once in phosphate-buffered saline solution (PBS), and resuspended in PBS to a final OD₆₀₀ of 1.0. Further dilutions were done in PBS. The number of bacterial cells in the injected sample was enumerated by plating 10-fold serial dilutions on LB agar plates and counting CFU after overnight incubation.

G. mellonella larvae (Vanderhorst Wholesale, Saint Mary's, OH) were used within 10 days of shipment from the vendor. Larvae were kept in the dark at 21°C before infection. Larvae weighing 200 to 300 mg were used in the LD₅₀ and survival assays as described previously (28), with slight modifications. Briefly, 5 μ l of the sample was injected into the last left proleg of the larvae using a 10- μ l glass syringe (Hamilton, Reno, NV) fitted with a 30G needle (Novo Nordisk, Princeton, NJ). Each experiment included control groups of noninjected larvae or larvae injected with 5 μ l sterile PBS. For rifampin experiments, approximately 30 min postinfection, worms were injected with 2 μ l of rifampin in the second-to-last left proleg using a 10- μ l glass syringe. Injected larvae were incubated at 37°C, assessing death at 24 h intervals over 6 days. Larvae were considered dead if they did not respond to physical stimuli. Experiments in which 10% or more of the larvae in either of the control groups died were omitted from the statistical analysis. Experiments were repeated three times using 10 or 20 larvae per experimental group.

The LD₅₀ for *A. baumannii* strains AB5075, ATCC 19606^T, and ATCC 17978 were determined by preparing a series of 2-fold dilutions of a PBS suspension of the bacterial strain, starting with a bacterial concentration that caused death of all the larvae within 24 h and going down to a concentration at which no deaths were recorded within this time frame. Twenty larvae were injected with 5 μ l of the appropriate dilution, and larvae were determined to be alive or dead after 24 h. Two independent

biological repeats of LD₅₀ determination were performed. LD₅₀ were determined using the Spearman-Kärber method.

Murine pulmonary model. The animal experimental procedures were approved by the Institutional Animal Care and Use Committee at the Walter Reed Army Institute of Research (IB02-10). All research was conducted in compliance with the Animal Welfare Act and other federal statutes and regulations relating to animals and experiments involving animals and adhered to principles stated in reference 39. Six-week-old female BALB/c mice (National Cancer Institute, Frederick, MD) were housed at 3 to 4 animals per cage and allowed access to food and water *ad libitum* throughout the experiment. The pulmonary infection model was adapted from reference 14. Briefly, to promote infection, mice were rendered neutropenic via intraperitoneal administration of 150 mg/kg and 100 mg/kg cyclophosphamide in sterile saline on day -4 and day -1 prior to infection (day 0), respectively.

A. baumannii isolates AB4857, AB5075, AB5711, AB0057, and AB5256 were grown overnight in LB broth with aeration at 37°C, subcultured to mid-exponential phase, washed, and resuspended in PBS with optical density at 600 nm (OD₆₀₀) values corresponding to 2×10^8 CFU/ml. For infection, mice were anesthetized with oxygenated isoflurane immediately prior to intranasal inoculation with 25 μ l of bacterial cultures, corresponding to 5×10^6 CFU. For rifampin experiments, mice were injected IP daily, starting at 4 h postinfection. Animal morbidity was scored twice daily for 6 days using a system evaluating mobility, coat condition, and conjunctivitis as previously described (14). As mice became exceedingly moribund based on clinical score, they were humanely euthanized according to protocol.

To assess CFU burden in the lungs, mice were humanely euthanized according to protocol on days 2 and 3 postinfection via an injection of ketamine (100 mg/kg) and xylazine (10 mg/kg). To quantify the pulmonary CFU burden, lungs were homogenized in 1 ml PBS, and serial dilutions were plated using the Autoplate spiral plating system (Advanced Instruments, Norwood, MA) onto LB agar supplemented with 50 μ g/ml carbenicillin. Bacterial load was reported as CFU per gram of lung tissue.

Transposon library generation. Transposon mutants were constructed using the EZ-Tn5 transposon construction vector pMOD-5<R6K γ ori/MCS> (Epicentre, Madison, WI). The transposable element was created by PCR amplifying *hph*, encoding hygromycin resistance, from vector pMQ300 (31) using the primers pMODHygForKPN (AAAAAAGGTACCGgaaatgtgctgcaacc) and pMODHygRevPST (AAAAAAC TGCAGTtggtctgacaatgatgcaattgg). The amplicon was then cloned into the multicloning site (MCS) of pMOD-5<R6K γ ori/MCS>. The transposome was constructed according to manufacturer's instructions and introduced into cells via electroporation. The transformed cells were selected for on LB agar supplemented with 250 μ g/ml hygromycin. Colonies were picked from plates and grown overnight in 96-well plates containing 100 μ l of low-salt LB supplemented with 250 μ g/ml hygromycin. After overnight incubation, 100 μ l of 50% glycerol was added to each well, and plates were immediately moved to -80°C for storage. The Tn5 mutant library was subjected to high-throughput sequencing as previously described (32).

Tn7-hyg construction and insertion onto the chromosome. To make Tn7-based genetic tools usable in AB5075, the *hph* gene, coding for hygromycin resistance, was cloned into pUC18T-mini-Tn7T-Zeo (40). Briefly, *hph* was amplified from pMQ300 (31) using primers pMOD Hyg For (AAAGCATGCGgaaatgtgctgcaacc) and pMOD Hyg Rev (AAAGC ATGCTtggtctgacaatgatgcaattgg) (lowercase indicates ●●●●) and ligated into pUC18T-mini-Tn7T-Zeo, which was digested with NcoI and then blunted with the Klenow fragment of the DNA polymerase I (Fermentas). A derivative of the pUC18T-mini-Tn7T-*hph* vector containing the *lux* operon was constructed by amplifying the *lux*ABCDE operon out of pUC18T-mini-Tn7T-Gm-*lux* (40) with the primers Lux For (TCAAGGT TCTGGACCATTG) and Lux Rev (AAAAAAAAGCTTGGTGTAGCGT CGTAAGCTAATA). The PCR product was digested with BamHI and HindIII and then cloned into the MCS of pUC18T-mini-Tn7T-*hph*.

The mini-Tn7 elements were transposed into the *attTn7* site of AB5075 via the method of Kumar et al. (41). Conjugation mixtures were scraped from LB plates, resuspended in 1 ml of PBS, and plated on LB agar supplemented with 250 $\mu\text{g/ml}$ of hygromycin and 25 $\mu\text{g/ml}$ of chloramphenicol. Insertion into the *attTn7* site was confirmed with the primers AB5075 *attTn7* FWD (AACACAAGTGGAAAGTGATTCT) and AB5075 *attTn7* REV (TGGCTTGACCAATCATTATAG), which flanked the *attTn7* site.

Statistical analyses All statistical analyses were carried out using GraphPad Prism version 5.01 for Windows (GraphPad Software, San Diego, CA). Survival curves were compared via Kaplan-Meier curve analysis with the Bonferroni correction for multiple comparisons. Recovered bacterial burdens were compared via either the Mann-Whitney U test or the Kruskal-Wallis test followed by Dunn's multiple-comparison test. All results were considered significant at a *P* value of <0.05 .

SUPPLEMENTAL MATERIAL

Supplemental material for this article may be found at <http://mbio.asm.org/lookup/suppl/doi:10.1128/mBio.01076-14/-/DCSupplemental>.

Figure S1A, TIF file, 0.6 MB.

Figure S1B, TIF file, 2.2 MB.

Figure S2, TIF file, 0.5 MB.

Table S1, DOCX file, 0.1 MB.

Table S2, DOCX file, 0.1 MB.

ACKNOWLEDGMENTS

We especially thank Brendan Corey for his technical assistance with the revised manuscript. We kindly acknowledge Colin Manoil for his collaboration in sequencing the Tn5 mutant library, his advice, and the critical reading of the manuscript. We thank Lenie Dijkshoorn for providing the clonal complex reference strains that were used as controls for the multiplex PCR assay. We are grateful to Robert Shanks for providing the gift of the pMQ300 plasmid. We thank COL Clint Murray and Mark Shirliff for providing two additional isolates from Brooke Army Medical Center. We are grateful to Herbert Shweitzer for providing the pUC18T-mini-Tn7T-Zeo plasmid, and Anthony Hay for providing the pUC18T-mini-Tn7T-Gm-lux plasmid.

The Zurawski laboratory and the research performed in this study were supported and funded via multiple grants from the Military Infectious Diseases Research Program (MIDRP) and the Defense Medical Research and Development Program (DMRDP).

The findings and opinions expressed herein belong to the authors and do not necessarily reflect the official views of the WRAIR, the U.S. Army, or the Department of Defense.

REFERENCES

- Pendleton JN, Gorman SP, Gilmore BF. 2013. Clinical relevance of the ESKAPE pathogens. *Expert Rev. Anti Infect. Ther.* 11:297–308. <http://dx.doi.org/10.1586/eri.13.12>.
- Dizbay M, Tozlu DK, Cirak MY, Isik Y, Ozdemir K, Arman D. 2010. In vitro synergistic activity of tigecycline and colistin against XDR-*Acinetobacter baumannii*. *J. Antibiot.* 63:51–53. <http://dx.doi.org/10.1038/ja.2009.117>.
- Murray CK, Hospenthal DR. 2008. *Acinetobacter* infection in the ICU. *Crit. Care Clin.* 24:237–248, vii. <http://dx.doi.org/10.1016/j.ccc.2007.12.005>.
- Hujer KM, Hujer AM, Hulten EA, Bajaksouzian S, Adams JM, Donskey CJ, Ecker DJ, Massire C, Eshoo RW, Sampath R, Thomson JM, Rather PN, Craft DW, Fishbain JT, Ewell AJ, Jacobs MR, Paterson DL, Bonomo RA. 2006. Analysis of antibiotic resistance genes in multidrug-resistant *Acinetobacter* sp. isolates from military and civilian patients treated at the Walter Reed Army Medical Center. *Antimicrob. Agents Chemother.* 50:4114–4123. <http://dx.doi.org/10.1128/AAC.00778-06>.
- Yun HC, Branstetter JG, Murray CK. 2008. Osteomyelitis in military personnel wounded in Iraq and Afghanistan. *J. Trauma* 64:S163–S168. <http://dx.doi.org/10.1097/01.ta.0000241143.71274.63>.
- Tong MJ. 1972. Septic complications of war wounds. *JAMA* 219:1044–1047. <http://dx.doi.org/10.1001/jama.219.8.1044>.
- Potron A, Munoz-Price LS, Nordmann P, Cleary T, Poirel L. 2011. Genetic features of CTX-M-15-producing *Acinetobacter baumannii* from Haiti. *Antimicrob. Agents Chemother.* 55:5946–5948. <http://dx.doi.org/10.1128/AAC.05124-11>.
- Wang T, Li D, Xie Y, Kang M, Chen Z, Chen H, Fan H, Wang L, Tao C. 2010. The microbiological characteristics of patients with crush syndrome after the Wenchuan earthquake. *Scand. J. Infect. Dis.* 42:479–483. <http://dx.doi.org/10.3109/00365541003671226>.
- Keen EF III, Murray CK, Robinson BJ, Hospenthal DR, Co EM, Aldous WK. 2010. Changes in the incidences of multidrug-resistant and extensively drug-resistant organisms isolated in a military medical center. *Infect. Control Hosp. Epidemiol.* 31:728–732. <http://dx.doi.org/10.1086/653617>.
- Evans BA, Hamouda A, Amyes SG. 2013. The rise of carbapenem-resistant *Acinetobacter baumannii*. *Curr. Pharm. Des.* 19:223–238. <http://dx.doi.org/10.2174/138161213804070285>.
- Lesho E, Yoon EJ, McGann P, Snesrud E, Kwak Y, Milillo M, Onmus-Leone F, Preston L, St Clair K, Nikolich M, Viscount H, Wortmann G, Zapor M, Grillot-Courvalin C, Courvalin P, Clifford R, Waterman PE. 2013. Emergence of colistin-resistance in extremely drug-resistant *Acinetobacter baumannii* containing a novel *pnrCAB* operon during colistin therapy of wound infections. *J. Infect. Dis.* 208:1142–1151. <http://dx.doi.org/10.1093/infdis/jit293>.
- Boucher HW, Talbot GH, Bradley JS, Edwards JE, Gilbert D, Rice LB, Scheld M, Spellberg B, Bartlett J. 2009. Bad bugs, no drugs: no ESKAPE! An update. *Infect. Dis. Soc. Am. Clin. Infect. Dis.* 48:1–12. <http://dx.doi.org/10.1086/591855>.
- de Brij A, Eveillard M, Dijkshoorn L, van den Broek PJ, Nibbering PH, Joly-Guillou ML. 2012. Differences in *Acinetobacter baumannii* strains and host innate immune response determine morbidity and mortality in experimental pneumonia. *PLoS One* 7:e30673. <http://dx.doi.org/10.1371/journal.pone.0030673>.
- Eveillard M, Soltner C, Kempf M, Saint-André JP, Lemarié C, Randrianarivelo C, Seifert H, Wolff M, Joly-Guillou ML. 2010. The virulence variability of different *Acinetobacter baumannii* strains in experimental pneumonia. *J. Infect.* 60:154–161. <http://dx.doi.org/10.1016/j.jinf.2009.09.004>.
- Smith MG, Gianoulis TA, Pukatzki S, Mekalanos JJ, Ornston LN, Gerstein M, Snyder M. 2007. New insights into *Acinetobacter baumannii* pathogenesis revealed by high-density pyrosequencing and transposon mutagenesis. *Genes Dev.* 21:601–614. <http://dx.doi.org/10.1101/gad.1510307>.
- Tomaras AP, Dorsey CW, Edelmann RE, Actis LA. 2003. Attachment to and biofilm formation on abiotic surfaces by *Acinetobacter baumannii*: involvement of a novel chaperone-usher pili assembly system. *Microbiology* 149:3473–3484. <http://dx.doi.org/10.1099/mic.0.26541-0>.
- Sahl JW, Johnson JK, Harris AD, Phillippy AM, Hsiao WW, Thom KA, Rasko DA. 2011. Genomic comparison of multi-drug resistant invasive and colonizing *Acinetobacter baumannii* isolated from diverse human body sites reveals genomic plasticity. *BMC Genomics* 12:291. <http://dx.doi.org/10.1186/1471-2164-12-291>.
- Loehfelm TW, Luke NR, Campagnari AA. 2008. Identification and characterization of an *Acinetobacter baumannii* biofilm-associated protein. *J. Bacteriol.* 190:1036–1044. <http://dx.doi.org/10.1128/JB.01416-07>.
- Ramirez MS, Don M, Merkié AK, Bistué AJ, Zorreguieta A, Centrón D, Tolmasky ME. 2010. Naturally competent *Acinetobacter baumannii* clinical isolate as a convenient model for genetic studies. *J. Clin. Microbiol.* 48:1488–1490. <http://dx.doi.org/10.1128/JCM.01264-09>.
- Russo TA, Beanan JM, Olson R, MacDonald U, Luke NR, Gill SR, Campagnari AA. 2008. Rat pneumonia and soft-tissue infection models for the study of *Acinetobacter baumannii* biology. *Infect. Immun.* 76:3577–3586. <http://dx.doi.org/10.1128/IAI.00269-08>.
- Vila J, Pachón J. 2012. Therapeutic options for *Acinetobacter baumannii* infections: an update. *Expert Opin. Pharmacother.* 13:2319–2336. <http://dx.doi.org/10.1517/14656566.2012.729820>.
- Adams MD, Goglin K, Molyneux N, Hujer KM, Lavender H, Jamison JJ, MacDonald IJ, Martin KM, Russo T, Campagnari AA, Hujer AM, Bonomo RA, Gill SR. 2008. Comparative genome sequence analysis of multidrug-resistant *Acinetobacter baumannii*. *J. Bacteriol.* 190:8053–8064. <http://dx.doi.org/10.1128/JB.00834-08>.
- van Belkum A, Tassios PT, Dijkshoorn L, Haeggman S, Cookson B, Fry NK, Fussing V, Green J, Feil E, Gerner-Smidt P, Brisse S, Struelens M, European Society of Clinical Microbiology and Infectious Diseases

- (ESCMID) Study Group on Epidemiological Markers (ESGEM). 2007. Guidelines for the validation and application of typing methods for use in bacterial epidemiology. *Clin. Microbiol. Infect.* 13(Suppl 3):1–46. <http://dx.doi.org/10.1111/j.1469-0691.2007.01786.x>.
24. Turton JF, Gabriel SN, Valderrey C, Kaufmann ME, Pitt TL. 2007. Use of sequence-based typing and multiplex PCR to identify clonal lineages of outbreak strains of *Acinetobacter baumannii*. *Clin. Microbiol. Infect.* 13: 807–815. <http://dx.doi.org/10.1111/j.1469-0691.2007.01759.x>.
 25. Zurawski DV, Thompson MG, McQueary CN, Matalka MN, Sahl JW, Craft DW, Rasko DA. 2012. Genome sequences of four divergent multidrug-resistant *Acinetobacter baumannii* strains isolated from patients with sepsis or osteomyelitis. *J. Bacteriol.* 194:1619–1620. <http://dx.doi.org/10.1128/JB.06749-11>.
 26. Rasko DA, Myers GS, Ravel J. 2005. Visualization of comparative genomic analyses by BLAST score ratio. *BMC Bioinformatics* 6:2. <http://dx.doi.org/10.1186/1471-2105-6-S2-S2>.
 27. Desbois AP, Coote PJ. 2012. Utility of greater wax moth larva (*Galleria mellonella*) for evaluating the toxicity and efficacy of new antimicrobial agents. *Adv. Appl. Microbiol.* 78:25–53. <http://dx.doi.org/10.1016/B978-0-12-394805-2.00002-6>.
 28. Peleg AY, Jara S, Monga D, Eliopoulos GM, Moellering RC, Jr, Mylonakis E. 2009. *Galleria mellonella* as a model system to study *Acinetobacter baumannii* pathogenesis and therapeutics. *Antimicrob. Agents Chemother.* 53:2605–2609. <http://dx.doi.org/10.1128/AAC.01533-08>.
 29. Manepalli S, Gandhi JA, Ekhar VV, Asplund MB, Coelho C, Martinez LR. 2013. Characterization of a cyclophosphamide-induced murine model of immunosuppression to study *Acinetobacter baumannii* pathogenesis. *J. Med. Microbiol.* 62:1747–1754.
 30. Dorsey CW, Tomaras AP, Actis LA. 2002. Genetic and phenotypic analysis of *Acinetobacter baumannii* insertion derivatives generated with a transposome system. *Appl. Environ. Microbiol.* 68:6353–6360. <http://dx.doi.org/10.1128/AEM.68.12.6353-6360.2002>.
 31. Kalivoda EJ, Horzempa J, Stella NA, Sadaf A, Kowalski RP, Nau GJ, Shanks RM. 2011. New vector tools with a hygromycin resistance marker for use with opportunistic pathogens. *Mol. Biotechnol.* 48:7–14. <http://dx.doi.org/10.1007/s12033-010-9342-x>.
 32. Gallagher LA, Ramage E, Patrapuvich R, Weiss E, Brittnacher M, Manoil C. 2013. Sequence-defined transposon mutant library of *Burkholderia thailandensis*. *mBio* 4:e00604–e00613.
 33. Antunes LC, Imperi F, Carattoli A, Visca P. 2011. Deciphering the multifactorial nature of *Acinetobacter baumannii* pathogenicity. *PLoS One* 6:e22674. <http://dx.doi.org/10.1371/journal.pone.0022674>.
 34. Gaddy JA, Arivett BA, McConnell MJ, López-Rojas R, Pachón J, Actis LA. 2012. Role of acinetobactin-mediated iron acquisition functions in the interaction of *Acinetobacter baumannii* strain ATCC 19606T with human lung epithelial cells, *Galleria mellonella* caterpillars, and mice. *Infect. Immun.* 80:1015–1024. <http://dx.doi.org/10.1128/IAI.06279-11>.
 35. Collinet-Adler S, Castro CA, Ledonio CG, Bechtold JE, Tsukayama DT. 2011. *Acinetobacter baumannii* is not associated with osteomyelitis in a rat model: a pilot study. *Clin. Orthop. Relat. Res.* 469:274–282. <http://dx.doi.org/10.1007/s11999-010-1488-0>.
 36. Thompson MG, Black CC, Pavlicek RL, Honnold CL, Wise MC, Alameh YA, Moon JK, Kessler JL, Si Y, Williams R, Yildirim S, Kirkup BC, Jr, Green RK, Hall ER, Palys TJ, Zurawski DV. 2014. Validation of a novel murine wound model of *Acinetobacter baumannii* infection. *Antimicrob. Agents Chemother.* 58:1332–1342. <http://dx.doi.org/10.1128/AAC.01944-13>.
 37. Buchan BW, McLendon MK, Jones BD. 2008. Identification of differentially regulated *Francisella tularensis* genes by use of a newly developed Tn5-based transposon delivery system. *Appl. Environ. Microbiol.* 74: 2637–2645. <http://dx.doi.org/10.1128/AEM.02882-07>.
 38. Jacobs MA, Alwood A, Thaipisuttikul I, Spencer D, Haugen E, Ernst S, Will O, Kaul R, Raymond C, Levy R, Chun-Rong L, Guenther D, Bovee D, Olson MV, Manoil C. 2003. Comprehensive transposon mutant library of *Pseudomonas aeruginosa*. *Proc. Natl. Acad. Sci. U. S. A.* 100:14339–14344. <http://dx.doi.org/10.1073/pnas.2036282100>.
 39. National Research Council. 2011. Guide for the care and use of laboratory animals, 8th ed. National Academies Press, Washington, DC.
 40. Choi KH, Gaynor JB, White KG, Lopez C, Bosio CM, Karkhoff-Schweizer RR, Schweizer HP. 2005. A Tn7-based broad-range bacterial cloning and expression system. *Nat. Methods* 2:443–448. <http://dx.doi.org/10.1038/nmeth765>.
 41. Kumar A, Dalton C, Cortez-Cordova J, Schweizer HP. 2010. Mini-Tn7 vectors as genetic tools for single copy gene cloning in *Acinetobacter baumannii*. *J. Microbiol. Methods* 82:296–300. <http://dx.doi.org/10.1016/j.mimet.2010.07.002>.